


# Graphene, an Interesting Nanocarbon Allotrope for Biosensing Applications: Advances, Insights, and Prospects

Biomedical Engineering and  
Computational Biology  
Volume 12: 1–19  
© The Author(s) 2021  
Article reuse guidelines:  
sagepub.com/journals-permissions  
DOI: 10.1177/1179597220983821



Farid Menaa<sup>1</sup> , Yazdian Fatemeh<sup>2</sup>, Sandeep K Vashist<sup>3,5</sup>,  
Haroon Iqbal<sup>5</sup>, Olga N Sharts<sup>1</sup> and Bouzid Menaa<sup>1</sup>

<sup>1</sup>Department of Nanomedicine and Fluoro-Carbon Spectroscopy, Fluorotronics, Inc and California Innovations Corporation, San Diego, CA, USA. <sup>2</sup>Department of Life Science Engineering, Faculty of New Sciences and Technologies, University of Tehran, Tehran, Iran. <sup>3</sup>Hahn-Schickard-Gesellschaft für Angewandte Forschung e.V. (HSG-IMIT), Freiburg, Germany. <sup>4</sup>Pictor Pvt. Ltd., 24 Balfour Road Parnell, Auckland, New Zealand. <sup>5</sup>College of Pharmaceutical Sciences, Soochow University, Suzhou, P.R. China.

**ABSTRACT:** Graphene, a relatively new two-dimensional (2D) nanomaterial, possesses unique structure (e.g. lighter, harder, and more flexible than steel) and tunable physicochemical (e.g. electrical, optical) properties with potentially wide eco-friendly and cost-effective usage in biosensing. Furthermore, graphene-related nanomaterials (e.g. graphene oxide, doped graphene, carbon nanotubes) have incited tremendous interest among scientists and industries for the development of innovative biosensing platforms, such as arrays, sequencers and other nano-optical/biophotonic sensing systems (e.g. FET, FRET, CRET, GERS). Indeed, combinatorial functionalization approaches are constantly improving the overall properties of graphene, such as its sensitivity, stability, specificity, selectivity, and response for potential bioanalytical applications. These include real-time multiplex detection, tracking, qualitative, and quantitative characterization of molecules (i.e. analytes [H<sub>2</sub>O<sub>2</sub>, urea, nitrite, ATP or NADH]; ions [Hg<sup>2+</sup>, Pb<sup>2+</sup>, or Cu<sup>2+</sup>]; biomolecules (DNA, iRNA, peptides, proteins, vitamins or glucose; disease biomarkers such as genetic alterations in BRCA1, p53) and cells (cancer cells, stem cells, bacteria, or viruses). However, there is still a paucity of comparative reports that critically evaluate the relative toxicity of carbon nanoallotropes in humans. This manuscript comprehensively reviews the biosensing applications of graphene and its derivatives (i.e. GO and rGO). Prospects and challenges are also introduced.

**KEYWORDS:** Graphene, nanocomposites, sensors, bioanalytical applications, innovation

**RECEIVED:** October 2, 2019. **ACCEPTED:** December 7, 2020.

**TYPE:** Review

**DECLARATION OF CONFLICTING INTERESTS:** The author(s) declared no potential conflicts of interest with respect to the research, authorship, and/or publication of this article. **Funding:** The author(s) received no financial support for the research, authorship, and/or publication of this article.

**FUNDING:** The author(s) received no financial support for the research, authorship, and/or publication of this article.

**CORRESPONDING AUTHOR:** Farid Menaa, Department of Nanomedicine and Fluoro-Carbon Spectroscopy, Fluorotronics, Inc and California Innovations Corporation, 2453 Cades Way, Bldg C, San Diego, CA 92081, USA. Email: dr.fmenaa@gmail.com

## Introduction

Carbon (C) nanomaterials (e.g. graphene (G), carbon nanotubes (CNTs), crystalline diamond, diamond-like carbon nanoparticles (CNPs), nanofibers) are continuously more sophisticated in their range of physicochemical tunable properties (e.g. 2D surfaces, 3D structures, porosity, stiffness, permeability, biocompatibility and biodegradability), and their diversity of use for biomedical and biochemical sensing applications (e.g. microbiology, environmental chemistry, oncology, regenerative medicine, tissue engineering, stem cell culture and maintenance) continues to expand, thereby providing potential opportunities to improve bioefficacy and biosafety<sup>1-6</sup> (Figure 1).

G (Figure 2) is one of the carbon allotrope which is also called “miracle material”<sup>2</sup> and is initially isolated almost 6 decades by Boehm et al<sup>7</sup> and Boehm and Hofmann,<sup>8</sup> who used transmission electron microscopy (TEM) and X-ray diffraction (XRD). This allotrope of carbon can be defined as a single planar sheet (i.e. flat monolayer carbon foils) of pure sp<sup>2</sup>-bonded carbon atoms densely packed into a 2D-honeycomb/hexagonal crystal lattice<sup>9-11</sup> G can be wrapped up into 0D fullerenes, rolled into 1D carbon nanotubes or stacked into 3D graphite (GP).<sup>10,12,13</sup>

About 15 years ago, the “Scotch tape” method (i.e. micro-mechanical exfoliation) employed by Geim and Novoselov allowed to produce large G sheets from GP. Briefly, this technique (Figure 3) used an adhesive tape to mechanically exfoliate bulk layered GP crystals into increasingly thinner pieces (i.e. 0.01 thousandth of an inch) in presence of silicon dioxide (SiO<sub>2</sub>) used as a “back gate” electrode to vary the charge density of G.<sup>14,15</sup>

Since then, the physicochemical (e.g. electrical, optical, mechanical, thermal and structural properties of G have been deeply studied.<sup>15-22</sup> All these studies contributed to scaling up production of sustainable, efficient and cost-effective quality G sheets.<sup>23-25</sup>

Innovative methods such as electrochemical reduction of exfoliated G oxide (GO) (which is oxidative and water-soluble form of G),<sup>5</sup> epitaxial growth in GP or in metals via chemical vapor deposition (CVD), facilitated this production<sup>26-32</sup> (Figure 4). In particular, G have excited many researchers and industries interested in developing nanobiosensors since Sir Geim and Sir Novoselov were awarded the 2010 *Nobel Prize* in Physics.<sup>33,34</sup> In recent years graphene and its derivatives like graphene oxide were shown to be most effective nanomaterials in applications of biomedical sciences.



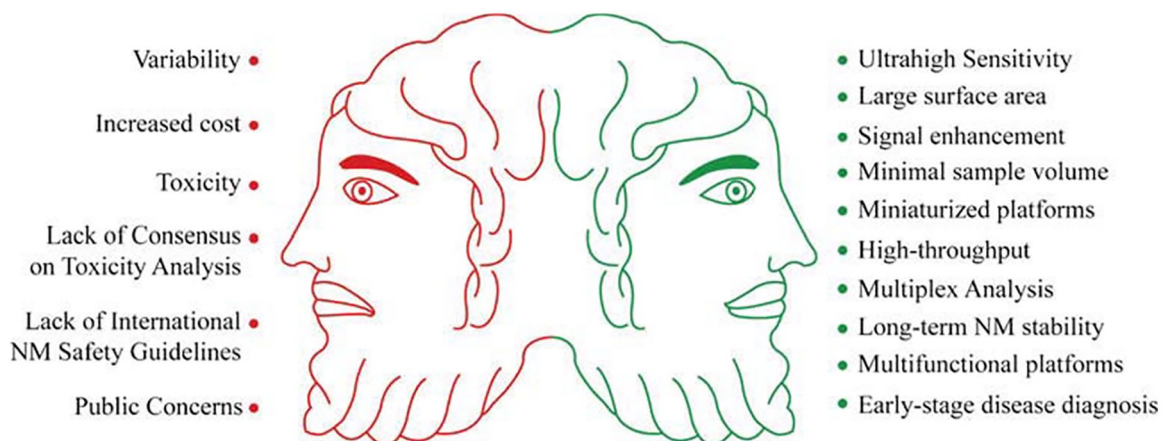


Figure 1. Nanotechnology-based diagnostics and biosensors: the 2 sides of the Janus.<sup>3</sup>

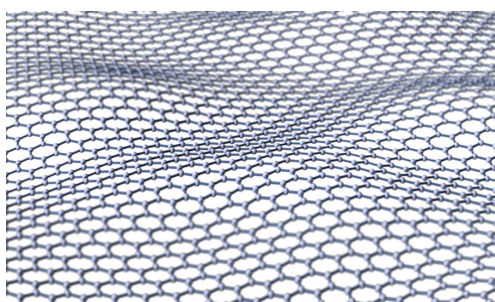


Figure 2. 2D structure of graphene.<sup>1</sup>

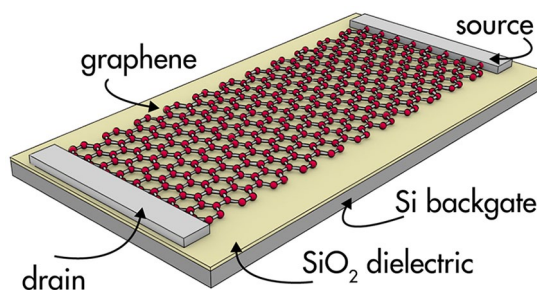


Figure 3. The "Scotch-tape" method.<sup>14,15</sup>

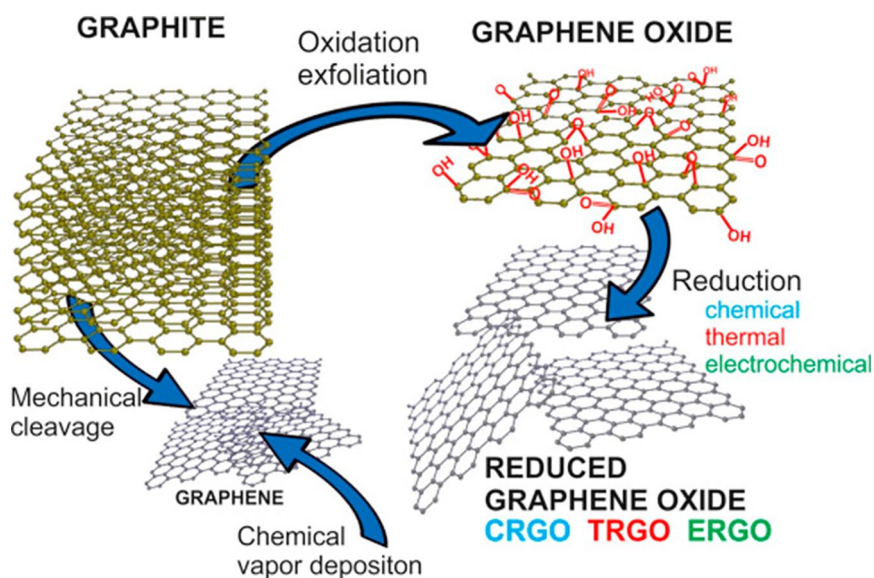


Figure 4. Production of graphene and derivatives by innovative processes.<sup>5,26-32</sup>

Although exceptional physicochemical properties and relative good safety *in vitro* are attributed to G and derivatives, their potential cell and systemic nontoxicity *in vivo* remain poorly defined.<sup>35,36</sup> Moreover, meta-analyses reporting benefits and risks (e.g. reliability, sensitivity, specificity, biocompatibility, biodegradability, toxicity) of carbon nanomaterials under specific conditions, will be an asset for the scientific community and industrials. For instance, *ab initio* calculations showed that

a G sheet with a size below 20 nm is thermodynamically unstable probably due to its lower-energy state at this condition.<sup>37,38</sup> Based on its physicochemical properties, large surface area and biocompatibility, graphene was thought to be utilized in stem cell-based tissue engineering.

Graphene is the nanomaterial most widely used for a variety of applications, introduced by Dresselhaus and Araujo.<sup>39</sup> The large specific area of graphene promotes the loading of

biomolecules in high concentrations on the sensing base to generate good detection sensitivity.<sup>40</sup> Its small band gap and high conductivity make easy conduction path of electrons between the graphene surface and the biomolecules. The highly pure graphene without any impurities and its derivative materials are inert in nature and are cost effective due to the superior uniform surfaces. Graphene's greatest sensing surface area augments the loading of targeted chemical species such as proteins and enzymes, either through submissive adsorption or through the chemical cross-linking to the analytes active groups.<sup>41</sup> The conductivity of graphene fluctuates depending upon the method of preparation or treatment. The electrical conductivity of graphene is 60 times more than single-walled carbon nanotubes (SWCNTs), while the measured electroconductivity of particulate graphene is 64 mS/cm as compared to graphene at 108 mS/cm.<sup>14,42</sup>

Graphene based sensors have pluripotent capacity for sensing a broad spectrum of molecules and ions. Due to chemical, electrical, electrochemical and optical properties of G, it is used as a sensor in diverse fields such as pressure sensor, strain gauge, biosensor, chemical sensor and gas sensor. The interaction G with dye molecules in G-dye hybrid optical sensors, leads to deep changes in the electronic structure of G which is suitable in various applications. These types of sensors can be used for sensing biomolecules and metal ions and synthetic molecules. Shetti et al used GO NPs fabricated on glassy carbon electrode (GCE) to analyze Congo red dye in the soil as well as in water samples. As a result, this application leads to water treatment from pollutants to be reuseable.<sup>27</sup>

All-G strain sensors are able to detect various types of strain induced via torsion, bending and stretching. Chun et al used introducing single-layer graphene as a force sensing material and with a conductive film composed of graphene flake for the electrode. The completed strain sensor can be fully flexible by using flexible materials.<sup>9</sup>

The 2D layers of sp<sup>2</sup> bonded carbon and 1-atom thick structure of G is useful as supporting material for metal and metal oxide catalyst NPs.<sup>10</sup> Using of metal oxides in sensor fabrication is growing rapidly due to their sensitivity, cost-effectiveness, chemical stability, non-toxicity, and rapid response.<sup>11</sup> For example, TiO<sub>2</sub>-loaded G as an electrochemical biosensor has been recently used. This combination has high electrocatalytic activity, biocompatibility, support enzyme immobilization, and direct electron transfer to enhance the electrochemical activity of the enzyme.<sup>10</sup> TiO<sub>2</sub> loaded G can be loaded with various materials such as hemoglobin,<sup>12</sup> glucose oxidase,<sup>13</sup> nickel foam<sup>14</sup> to some types of detections. ZnO is another metal oxide which is using in combination of G in biosensors. Various inherited properties of ZnONPs have allowed the successful immobilization of different types of biomolecules on their surfaces.<sup>15</sup> Gao et al used ZnO nanowire arrays with G and G foam to detect folic acid.<sup>16</sup> Electrochemical sensors have unique properties especially in biomedical research and are

used widely. Modification of conducting polymers with metal oxides, metal particles and carbon materials improve its stability, reproducibility and sensitivity which have effect on sensor performance. Conducting polymers are extensively used in electrochemical biosensors.<sup>11</sup> G and GO are rich in oxygen functional groups that act as a catalysis to develop different types of biosensors and have effect on surface functionalization, the attachment of biological recognition element and compatible with micro/nano-bioenvironment. So, G-based electrochemical biosensors are useable in monitoring noncommunicable diseases such as acute myocardial infarction, lung cancer, asthma, and diabetes detection.<sup>17</sup>

Both 3D graphene and reduced GO are broadly utilized as sensor devices and such graphene materials dispersion on the sensing surface is habitually accomplished by dropcast of suspension of graphene and its derivatives. Multifunctional components such as polymers could also be designed to coat to the graphene nanohybrid-modified electrode bases. The methods of noncovalent graphene hybridization with a polymer or small organic molecules should be carefully undertaken, as added raw materials may display an intrinsic electrochemistry or an interfere with the desired properties. However, chitosan, a biocompatible organic material, has the ability to disperse graphene and allow bioconjugation to build sensitive biosensors. Graphene-based electrochemical sensors can be used more easily than conventional methods, such as that of spectrometers.<sup>43-45</sup> Additional advantages are the flexibility, resistance, conductivity, and stability. These features are used in the advancement of various types of sensors to detect biological-important molecules. Pure forms of graphene, oxide and biocomposites have been customized with nanofibers, nanocubes, and other geometrical NPs, for the development of sensors for glucose.<sup>45-48</sup> The combination of hydrogen peroxide (H<sub>2</sub>O<sub>2</sub>) with graphene sensors is 1 more area that has drawn attention in recent years. The intrinsic changed and doped graphene (N-graphene) materials showed the best electrocatalytic response toward H<sub>2</sub>O<sub>2</sub>. Photodetectors, temperature sensors, and radiofrequency applications are additional uses of graphene-based sensors. Graphene is used in the form of nanowires, nanoribbons, and also some others arrays of NPs.<sup>49</sup>

Since detection of nitrite is important for environmental safety and human health, development of high-performance sensors for accurate detection of nitrite is highly desirable. Zhou et al designed and fabricated a highly sensitive graphene electrochemical transistor (GECT) nitrite sensor. AuNPs modified rGO nanocomposites (AuNPs/RGO) and used to improve its performance.<sup>18</sup> In another study, AuNPs-decorated on single-layer G (AuNPs/SLG) with good dispersion and clean surface promoted immobilization of glucose oxidase (GOD) in glucose biosensor.<sup>19</sup> GO is also useable in drug determination. To detect hydrochlorothiazide (HCT) at GO NPs modified GCE, an electro-oxidation process was developed. GO NPs influenced voltammetry behavior of diagram.<sup>20</sup>



It is obvious that detection of some analytes with low charge and small molecules is challenging. To solve this problem, a label-free G-field effect transistor (FET) biosensor with overly sensitive in detection the electric-neutral and low molecular weight ligands by using GR as probe was used.<sup>21</sup> In some studies, the incorporation of G with clay particles for using in sensors has been reported. This combination improves mechanical properties of G and offers functionality to the clay-G nanocomposites. Additionally, this composite has ability for analysis of target molecules including drug release monitoring and improve absorption. G-clay hybrid based are used in electrochemical sensors, gas sensors and biological sensors (glucose/ $H_2O_2$ ).<sup>22</sup> Wang et al developed a 3D hollow quasi-graphite capsules/polyaniline hybrid to sense ammonia gas at room temperature.<sup>23</sup> Since GO has electrical, physical and chemical properties with excellent chemical stability, it become an ideal candidates for gas sensing.<sup>24</sup> Shetti et al used GO and nanoclay composite-modified carbon paste electrode for the detection of theophylline for healthcare application. To test the applicability of the electrode, it was used to pharmaceutical and urine sample analysis.<sup>27</sup> In another study, GO was blended with carbon paste matrix and then fabricated GO-CPE was utilized as a sensor for flufenamic acid (FFA) quantification. In the following, the analytical application of this chemically modified electrode was used in determination of FFA in urine samples.<sup>26</sup> G quantum dots (GQDs) are zero-dimensional G nanostructures that have few layers or a SLG < 100 nm and are highly promising candidates for many applications such as sensing.<sup>27</sup> Mycotoxins are secondary toxin metabolites that produced from organisms of fungus and cause diseases and even death in humans and animals.<sup>28</sup> Lu et al reported detection of fumonisin B1 and deoxynivalenol as types of mycotoxin, by using carbon electrode modified with AuNPs and polypyrrole electrochemically rGO.<sup>29</sup>

Strong interactions between CNT and GO via  $\pi$ - $\pi$  stacking leads to a steady hybrid with definite specifications, together with high specific area, conductivity, performance, and good catalytic activity. Several research groups reported the fabrication of GO-CNTs nanohybrids as well as their potential applications.<sup>50</sup> Tian et al<sup>51</sup> synthesized stable SWCNT and GO hybrid composite through ultrasonication. Kim et al<sup>52</sup> fabricated GO-SWCNTs nanohybrid-coated glassy carbon electrodes (GCE) and utilized them as an anode for solar polymorphic cells. L-Lyrosine was electrochemically determined at GO-CNT-modified GCE by Li et al.<sup>53</sup> Rutin was detected by using voltammetric methods at MWCNT and laminate rGO composite modified GCE sensor by Zhu et al.<sup>54</sup> The complete electrochemistry of horseradish peroxidase was understood by Zhang et al<sup>55</sup> with an electrode modified with GO and MWCNT nanocomposite. Thus, nanocomposites of GO-CNT have potentially large applications in the fabrication of modified electrodes and investigation of biomolecules.

This manuscript analyses breakthroughs in G-based biosensing research. It also outlines perspectives and challenges in translational nanomedicine.

## Graphene and Graphene Derivatives: Malleable Giants Nanomaterials!

### *Isolation of G and G derivatives*

Synthesis of high-quality G is key to realization and controlling G physical and chemical properties. Among different methods of G synthesis, CVD and the exfoliated synthesis of G from graphite (GP) have become useful for the large-scale synthesis of G. In CVD method, G was prepared using methane as the carbon source on copper foils. Scanning electron microscopy (SEM) images show that CVD is a very suitable method to make highly pure and controlled number of layers of G sheets with a low O/C ratio which is require for a better performance of G.<sup>30</sup> In the liquid phase exfoliation (LPE) process, GP is exposed to liquid medium and single layer of graphitic plane is peeled off. Nowadays, experiments have shown that LPE is a much easier process to make G with high stability compared to other strategies. In this method, to counter the interfacial interaction between the GP layers and to stabilize G, a proper organic solvent with strong binding power to the graphitic plane was employed.<sup>31</sup>

Historically, GP oxide reduction/exfoliation (e.g. by hydrazine ( $N_2H_4$ ) reflux and rapid heating) was probably the first method used to synthesize monolayer flakes/films of G, as reported by Boehm et al<sup>7</sup> and Boehm and Hofmann.<sup>8</sup> Then, in 2004, high quality G sheets from bulk-GP were obtained by the "scotch tape" technique.<sup>14</sup> This technique was simplified in 2005 using the drawing method for "dry deposition," thereby avoiding the stage when G floated in a liquid.<sup>11</sup> In 2006, soluble fragments of G have been prepared through chemical alteration of GP.<sup>56</sup> Briefly, microcrystalline GP was first treated with a strong acidic mixture of sulfuric acid ( $H_2SO_4$ ) and nitric acid ( $HNO_3$ ). A series of steps involving oxidation and exfoliation resulted in small G plates with COOH groups at their edges. These groups were converted to hydrogen chloride (HCl) groups by treatment with thionyl chloride ( $SOCl_2$ ). Next, they were converted to the corresponding G amide via treatment with octadecylamine ( $C_{18}H_{37}NH_2$ ). The resulting material (i.e. circular G layers of 5.3 Å (Angstrom) thickness was soluble in tetrahydrofuran ( $C_4H_8O$ ), tetrachloromethane ( $CCl_4$ ), and dichloroethane ( $C_2H_4Cl_2$ ).

However, partial removal (< 80%) of various functional groups (e.g. COOH) in G, by reduction methods in solvents ( $N_2H_4$  stirring with HCl;  $SOCl_2$ ), has hampered its quality due to generated instability. Recently, it was reported reduction and exfoliation of GP oxide with lesser oxygen functionalities by focused solar radiation.<sup>57</sup>

In 2007, thin graphitic films using exfoliation techniques similar to the drawing method, and multilayer samples down to

10 nm in thickness, were obtained.<sup>10,14</sup> Jian et al developed a catalytic chemical vapor deposition route for the synthesis of 3D GP-like capsules with unique thickness and morphology control. The 3D GP-like capsules disperse well and show good structural stability.<sup>32</sup>

### *Graphene with CNTs, G-C3N4*

Graphitic carbon nitride (g-C3N4), as a novel metal-free 2D semiconductor material, has attracted public attention recently. Due to its characteristics of unique optical and electrical properties, layered structure, high chemical and thermal stability, excellent biocompatibility and low toxicity, g-C3N4 has been widely used in photocatalysis,<sup>33-35</sup> bioimaging,<sup>36,37</sup> electrocatalysis,<sup>38,39</sup> and biosensing.<sup>40-42</sup> However, the pure g-C3N4 has some limits such as high recombination rate of photogenerated carriers, narrow light absorption range and low specific surface areas. Accordingly, there are several approaches emerged to overcome the drawbacks, including doping photoactive elements, copolymerizing with electron-enriched molecules, adjusting the shape to form small-size nanostructure and establishing heterojunction with proper materials.<sup>43-45</sup> Among all, establishing heterojunction is a facile and efficient way to improve the performance of g-C3N4. Mazhabi et al designed a label-free PEC aptamer-based on g-C3N4/AgI nanocomposite for the specific detection of cancer cells, which significantly enhanced the photocurrent response of pure g-C3N4.<sup>46</sup>

Recently, carbon nanotubes (CNTs) have been used in the field of cancer diagnosis and therapy. Compatibility with biological systems, probability of variable functionalization, and the thermodynamic properties of CNTs are the main reasons for vast investigations.

The studies on cancer therapies are divided into 2 main categories based on the conducted therapy strategies, which include targeted drug delivery systems (DDS), and thermal ablation. Using chemical conjugation was the crucial part of the studies in both groups. Classification of the cancer therapy studies based on the cancer type, and introducing the novel strategies developed for both diagnosis and treatment of cancer is a challenge.

CNTs are one of the most commonly used NPs for cancer therapy. CNTs are categorized into 3 main types of SWCNTs, multi-walled CNTs (MWCNTs) and double-walled CNTs (DWCNTs).<sup>47</sup> CNTs are utilized in both cancer diagnosis and therapy; one of the first reviews in this matter was written by Yang et al<sup>48</sup> in which CNT was admired as an improving agent for cancer diagnosis because of properties like large surface, conjugation ability and encapsulation of drugs. Srivastava et al<sup>49</sup> investigated the effects of MWCNTs on the cellular scale. The noncytotoxic concentrations of CNTs were used in a lung cancer cell line (A549) and the apoptotic processes of the cells were analyzed. The desoxyribonucleic acid (DNA) laddering, nuclear condensation, and the changes in expression

of apoptotic biomarkers have been among the tests confirming higher apoptosis in cancer cell lines. Furthermore, the production of reactive oxygen species (ROS) was observed, accompanied by a decrease in activity of catalase and glutathione. Some studies were conducted through a combination of CNTs and bioactive compounds.

### *Morphological and Physicochemical Properties of G*

**Structure and molecular stability.** G is a fascinating allotrope of pure sp<sup>2</sup>-bonded carbon atoms densely arranged in a regular hexagonal crystal lattice pattern similar to GP but in a single planar sheet.<sup>9,10</sup> Therefore, it is considered as the limiting case of the polycyclic aromatic hydrocarbons' family (Figure 2).

G is a building block for graphitic materials. For instance, it can be wrapped up into 0D fullerenes, rolled into 1D nanotubes or stacked into 3D GP.<sup>12,24</sup> However, the irregular, impure and faulty shapes and sizes of G sheets in these devices are undesirable for applications, questioning the 2-dimensionality of G.<sup>58</sup> Indeed, suspended flat sheet of G showed ripples, with amplitude of about 1 nm, that may be either intrinsic to G (e.g. thermal instability/fluctuations), or extrinsic (e.g. ubiquitous dirt seen in all TEM images).<sup>56,59,60</sup> Interestingly, G can self-repair holes in G sheets when submitted to carbon molecules (e.g. hydrocarbons) or pure carbon atoms.<sup>61</sup>

TEM on sheets of G suspended between bars of a metallic grid revealed the structure of single-layer G (SLG).<sup>62</sup> G is light (about 0.77 mg m<sup>-2</sup>) but strong, flexible thanks to its gate-tunable planar structure which displays a large surface area. The carbon-carbon (C-C) bond length in G is about 0.142 nm.<sup>20</sup> G sheets stack to form GP with an interplanar spacing of 0.335 nm.<sup>63</sup> Altogether, the data showed that G represents an ideal molecular substrate. Besides, it is also possible to obtain real-space atomic resolution images of isolated SLG on SiO<sub>2</sub> substrates by scanning tunneling microscopy (STM). Importantly, rippling of G on the SiO<sub>2</sub> surface was determined to be caused by conformation of G to the underlying SiO<sub>2</sub>, and not an intrinsic effect.<sup>64,65</sup> More recently, the atomic structure of G was further revealed by atomic force microscopy (AFM), correlated between the amount of deposited DNA and the G layer thickness and the resulting π-π stacking/electrostatic interaction of ssDNA with G correlated between the amount of deposited DNA and the G layer thickness and was proved better than SiO<sub>2</sub> in absence of screening deposition.<sup>21</sup>

Through *ab initio* calculations, G sheet < 20 nm (< 24 000 C) is thermodynamically unstable with a tendency to scroll and buckle probably due to its lower-energy state. However, intrinsic microscopic roughening on the scale of 1 nm could stabilize pure 2D crystals.<sup>37,38,66</sup>

**Electronic and optical properties.** Much attention has been devoted to G due to its extraordinary electronic properties, especially on electron mobility, and this is having a beneficial impact on optoelectronic and nanoelectronic applications (e.g.

sensors). Indeed, G was firstly defined by Wallace as a zero-gap semiconductor, which limited some applications (e.g. building of logic circuits in G-FETs).<sup>67-71</sup> Nevertheless, it has been reported more recently that the quantum capacitance (gate potential), assessed by a three-electrode electrochemical configuration, has a non-zero minimum at the Dirac (corner) point, but that ionized impurities (low K, dopants) would influence this gate potential.<sup>71</sup> In fact, G exhibits a fast electron mobility (i.e. up to  $40\,000\text{ cm}^2\cdot\text{V}^{-1}\cdot\text{s}^{-1}$  for G on  $\text{SiO}_2$  substrates) at room temperature which besides is also explained by its low resistivity (i.e.  $10^{-6}\ \Omega/\text{cm}$ ).<sup>10,58,72</sup> This mobility can even reach approximately  $70\,000\text{ cm}^2\cdot\text{V}^{-1}\cdot\text{s}^{-1}$ , depending on the dielectric constant, when transport properties of G-FETs are evaluated in different solvents. Interestingly, bilayer G (BLG) produced by CVD displayed tunable band gap (quantum hall effect) and a potential for excitonic condensation.<sup>73-76</sup>

The optical features of G is mainly characterized by a high opacity, which in SLG enables a weak absorbance (2.3%) of white light, a tunable and ultrafast response, a non-linear optical behavior (i.e. saturable absorption under strong excitation over the visible to near-infrared (NIR) region).<sup>17,18,77-80</sup> Thereby, G/GO system displayed electrochromic behavior, tunable and ultrafast optical response. Further, G nanoribbons, resulting of G-cut CNTs, elicited optical tunability into the terahertz (THz) regime when a magnetic field was applied.<sup>18,78</sup> Few years ago, a study using prism coupling technique showed that a 1D photonic crystal namely G-based Bragg grating was capable of exciting surface electromagnetic waves.<sup>81</sup>

Taken together, G offers wide applications in ultrafast photonics (e.g. sensors, mode locking of fiber lasers, microwave and THz photonic devices).<sup>79,80,82</sup> High thermal stability, admirable conductivity and large surface area are making laser-induced graphene foam (LIGF) as an interesting material in recent researches. Aslam et al used this characteristic and developed a strategy to use LIGF directly as anode material in lithium ion batteries.<sup>50</sup>

**Mechanical and thermal properties.** The mechanical properties of G are amazing. Indeed, G has a breaking strength of over 100 times greater than a hypothetical steel film of the same thickness, as well as a stiffness of 1 terapascal (TPa) which represents  $150\,000\,000\text{ psi}$ .<sup>83</sup> The Casimir effect of G (i.e. interaction between any disjoint neutral bodies provoked by the fluctuations of the electrodynamic vacuum in G systems) was quite surprising, and demonstrated the great interaction of G with the electromagnetic field.<sup>84,85</sup> This interaction was mediated by an unusual van der Waals/dispersion force since its obeyed to an inverse cubic asymptotic power law, and not to the usual inverse quartic.<sup>86</sup>

Besides, the thermal conductivity of G was phonon-dominated, isotropic, and ranged between  $4.84 \pm 0.44 \times 10^3$  and  $5.30 \pm 0.48 \times 10^3\text{ W}\cdot\text{m}^{-1}\cdot\text{K}^{-1}$ .<sup>87,88</sup>

### *Qualitative and Quantitative Enhancements of Graphene (G)*

In the recent years, the overall breakthroughs helped to attract attention from many research groups that aimed to scale up quality and lead to sustainable and cost-effective production of G.<sup>10,23,25</sup> This will have an increasing impact on the design and development of innovative biomedical and biochemical applications.<sup>89-92</sup> Indeed, various innovative processes were used, including layer-by-layer (LbL) self-assembly, reduction of GO (rGO), epitaxial growth either in GP containing silicon carbide (SiC) or in metals as substrates (e.g. iridium [Ir], gold [Au]), transition metal-carbon melting (e.g. nickel [Ni], copper [Cu]), cut CNTs to obtain G-nanoribbons, pyrolysis of sodium ethoxide, GP sonication, or carbon dioxide ( $\text{CO}_2$ ) reduction.<sup>93-103</sup>

Thereby, transparent (i.e. with 80% of light transmittance), resistant (with  $1.4\text{ k}\Omega/\text{sq}$ ), and electrically-enhanced G thin films were easily manufactured using LbL assembly process, which was based on electrostatic interactions (i.e. alternate LbL deposition of oppositely charged G nanosheets) in an aqueous thermally-controlled environment.<sup>26</sup> In such study, amine ( $\text{NH}_2$ )-functionalized G (+) nanosheets (i.e. produced by amidation) and carboxylic acid ( $\text{COOH}$ )-functionalized G (-) nanosheets (i.e. produced by acyl-chlorination via the use of thionyl chloride) resulted from the reduction of GO pre-obtained from GP powder using Hummer's method (see Section I.4.). Furthermore, a facile, fast, clean and green method for large-scale synthesis of high-quality G nanosheets has been described, which employed the electrochemical reduction of exfoliated GO precursor at drastically reduced cathodic potentials, and this permitted smallest electron transfer rates (ETR) compared to that on a GCE.<sup>28,29</sup> Alternative unconventional methods have also been described. These include modification of G sheets by pyrene-grafted polyacrylic acid (PAA) in aqueous solution, LbL alternating deposition with polyethylenimine (PEI) as well as techniques based on nanocomposites hybridization with G (e.g. decoration of G self-assembly achieved by electroless deposition of Au NPs using Cu substrate as a source of electrons).<sup>93,94,97</sup> Besides, quasi-free-standing epitaxial G on SiC has been obtained by hydrogen intercalation from ultra-thin graphitic films when heating SiC to over  $1100^\circ\text{C}$  under low pressures (ca.  $10^{-6}\text{ torr}$ ).<sup>30,31</sup> Several key features of G have been identified by this process, such as the first visualization of electronic band-structure that is "Dirac cone" structure, or the massless Dirac fermions (i.e. anomalous "quantum Hall" effect).<sup>104-107</sup>

Depending on the symmetry, surface purity, thickness uniformity and nature of the interlayer interactions, the electronic properties of certain epitaxial multi-layered G (MLG) can be affected.<sup>105,108,109</sup> Indeed, although the band gap of the epitaxial G can be tuned by laser beam irradiation, many ripples and subsequent minigaps in the electronic band-structure have been noticed depending on the substrate. For instance, on Ir111, G was very weakly bonded, uniform in thickness, but



was slightly rippled and this was affecting its conductivity.<sup>110</sup> More recently, G on Au111 is looked as one of the most suitable alternative material because of its highly conductivity and excellent adsorption properties useful for high-resolution biosensing.<sup>111</sup>

Likewise, the epitaxial growth of G on noble metals, the production of G is also possible from metal-carbon melts. The general idea in this process is to dissolve carbon atoms inside a transition metal melt at a certain temperature, and then allow to precipitate out at lower temperatures. Among the transition metals, Ni28 provides a better substrate for growing SLG.<sup>112</sup> Indeed, Ni is not Raman active and so, the direct Raman spectroscopy of G layers on top of Ni is achievable. Therefore, high-quality SLG exceeding 1 cm<sup>2</sup> (0.2 sq inches) in the area, as well as MLG, have been synthesized using CVD on thin Ni, at low pressures and at temperatures compatible with conventional complementary metal oxide semiconductor (CMOS) processing (i.e. a technology for constructing integrated circuits). Usually, either Ni-based alloy with Au is used as catalysts or Cu films with low concentrations of methane (CH<sub>4</sub>) as a carbon source.<sup>113,114</sup> It is interesting to note that larger hydrocarbon gases (i.e. ethane [C<sub>2</sub>H<sub>6</sub>], propane [C<sub>3</sub>H<sub>8</sub>]), usually induce growth of BLG. All these sheets have been successfully transferred to various substrates, demonstrating viability for numerous electronic applications, including biosensing.<sup>25,113,115</sup>

Moreover, the production of G nanoribbons confers them certain electrical properties. This production can be made from MWCNTs cut open in solution by action of potassium permanganate (KMnO<sub>4</sub>) and sulfuric acid (H<sub>2</sub>SO<sub>4</sub>), or by plasma etching of CNTs partly embedded in a polymer film.<sup>116,117</sup>

Depending on the width of unbounded edges, G nanoribbons can either be configured in zigzag (i.e. metallic and semi-conducting “nanostripes”) or armchair (i.e. semi-conducting nanostructures).<sup>118,119</sup> More recently, large quantities of width controlled G-nanoribbons have been produced via GP nanotomy process.<sup>120</sup> The 2D structure, high electrical and thermal conductivity, and low noise of G nanoribbons represent a possible alternative to Cu for integrated circuit interconnects. There is besides an enormous excitement to create GQD (i.e. quantum confinement), which is possible by changing the width of G nanoribbons at select points. G-QDs consist of a single atomic layer of nano-sized GP (SLGP) and display excellent performances of G (e.g. better surface grafting using  $\pi$ - $\pi$  conjugation and surface groups, superior chemical inertness, higher biocompatibility and lower toxicity).<sup>121-123</sup>

Gram-quantities of G have been obtained through ethanol reduction by sodium metal followed by pyrolysis of the ethoxide product, and subsequent water washing to remove sodium salts. Furthermore, G can be obtained by GP sonication and centrifugation in N-methylpyrrolidone (NMP) solution or other suitable ionic liquid.<sup>67,99,124,125</sup>

Eventually, a scalable production of single to few layer pure G nanosheets up to 10 atoms thick that employed an exothermic combustion reaction of certain Group I and II metals,

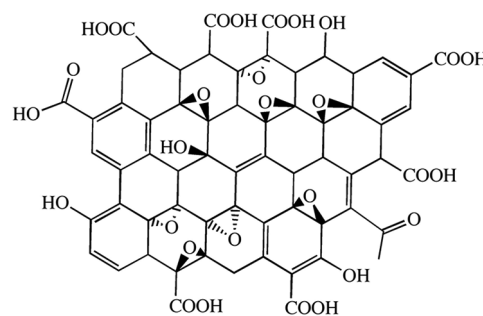


**Figure 5.** 2D structure of graphene oxide.<sup>51</sup>

including magnesium (Mg), and carbon bearing gases (e.g. CO<sub>2</sub>), has been reported by Graphene Technologies (Novato, CA, USA) and Hosmane’s research group.<sup>103</sup>

### *Graphene Oxide (GO): A Major Graphenic Derivative!*

GO (Figure 5) is routinely resulting from G oxidation using Hummer’s method, which involves a combination of KMnO<sub>4</sub>, sodium nitrate (NaNO<sub>3</sub>), H<sub>2</sub>SO<sub>4</sub>.<sup>126</sup> It is worth noting that the degree of oxidation as well as the chemical surface functionalization of GO may influence the electrical conductivity.

An improved GO synthesis route reported by Marcano et al<sup>127</sup> excluded NaNO<sub>3</sub>, increased the amount of KMnO<sub>4</sub>, and performed the reaction in a 9:1 mixture of H<sub>2</sub>SO<sub>4</sub>/phosphoric acid (H<sub>3</sub>PO<sub>4</sub>) in the presence of N<sub>2</sub>H<sub>4</sub>. This new method not only improved the efficiency of oxidation (i.e. greater amount of hydrophilic GO), but also avoided the generation of toxic gas while better controlling the temperature. Although this process might facilitate large-scale production of GO, the electrical conductivity of GO Marcano’s method was like that of Hummer’s method. Also, both Hummer’s and Marcano’s methods are time-consuming and present a risk of slash sheets into small pieces and/or occurrence of nm-sized holes in the basal plane. To overcome these limiting factors that could compromise the construction of original biosensors, Chiu et al<sup>128</sup> has reported an extraordinary fast and scalable approach that intentionally removed KMnO<sub>4</sub> from the process, and used microwave heating to combine its unique properties with aromatic oxidation by nitronium ions (NO<sub>2</sub><sup>+</sup>). Eventually, it worth noting from Boehm’s titration that SLG oxide (SLGO) undergoing high temperature chemical treatment resulted in sheet folding and loss of carboxylic functionality.<sup>129</sup> Alternatively, SLGO undergoing room temperature treatment with carbodiimides led to the collapse of individual sheets into star-like clusters, which exhibited poor reactivity with amines and potentially limited their use in composite synthesis.<sup>130</sup>

### *Graphene and Derivatives: Trends and Prospects in Biosensing Applications*

**Current status: A road to functionalized graphene!** From diagnosis of life-threatening diseases to detection of biological agents,

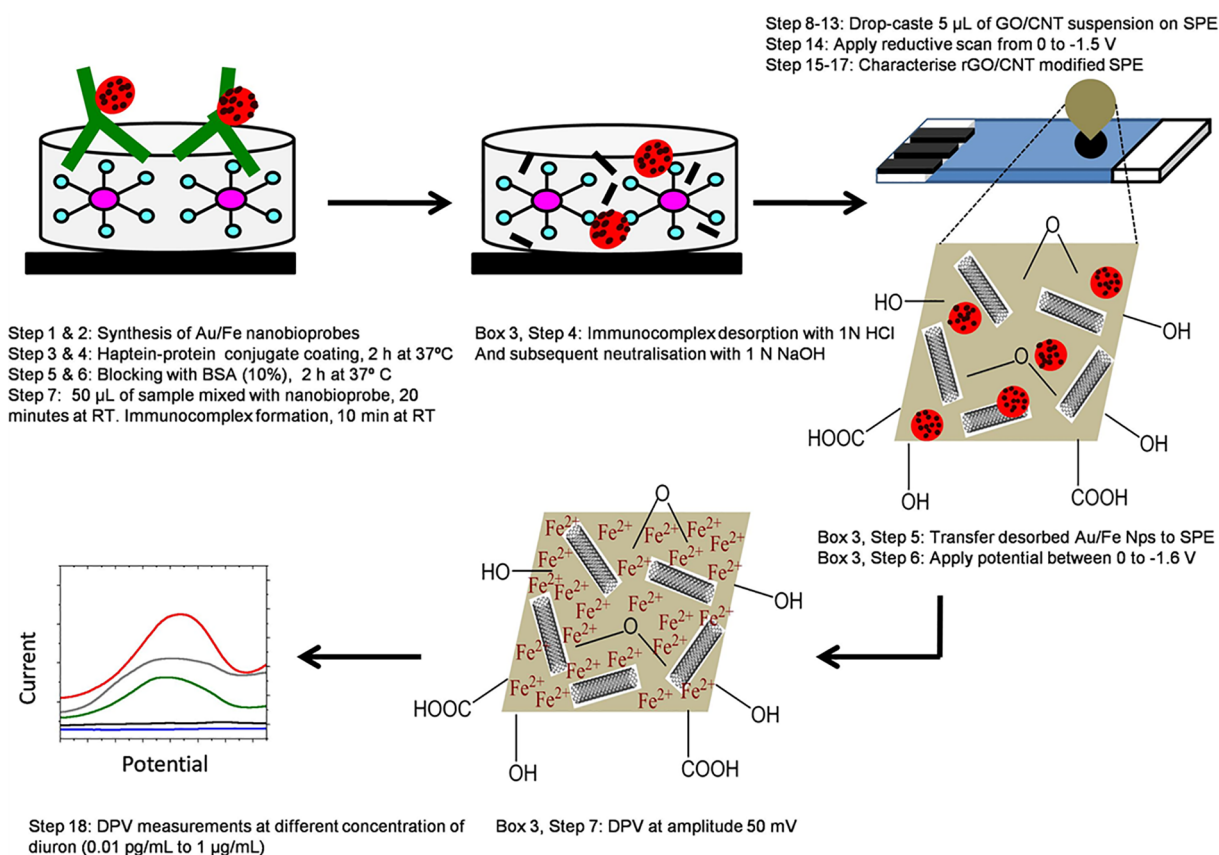


Figure 6. Example of a graphene-based biosensor.<sup>52</sup>

nanocarbon allotropes-based biosensors are becoming a critical part of modern life. From the reasons previously evoked, which include large surface area and excellent electrical conductivity, (original or functionalized) G is a nanomaterial of choice for electrochemical and optical biosensing over CNTs.<sup>131-135</sup> The functionalization of G films and GO hybrid nanocomposites (Figure 6) by chemical (e.g. decoration with noble metals), physical (e.g. ionic liquid) or biological (e.g. doping with peptides or proteins) procedures is important to regulate their electronic properties better, facilitate molecular interactions, and strengthen their interfaces with matrices.<sup>130,136-139</sup>

In the detection of single or multiplexed biomolecules, when G or derivatives (e.g. GO, GO-based hybrid nanocomposites, rGO) act as “electron wires” between the redox centers of a protein or an enzyme (e.g. *horseradish peroxidase* (HRP), glucose oxidase [GOD]) and an electrode’s surface (e.g. GCE), it was observed high accuracy, stability, sensitivity, specificity.<sup>140,141</sup> Such systems were useful for nucleotides and amino acids, DNA including genetic alterations, interference ribonucleic acid (iRNA), peptides or proteins including protein markers of diseases, glucose, biochemicals (e.g. hydrogen peroxide ( $\text{H}_2\text{O}_2$ ), NADH, urea, adenosine triphosphate (ATP), vitamins, chemicals (e.g. metals ions such  $\text{Cu}^{2+}$  or  $\text{Hg}^{2+}$ , as well as a number of living cells such mammalian cells or bacteria.<sup>41,142-158</sup>

Furthermore, photo-conducting properties of GO flakes in polymers were higher than unmodified GO.<sup>159</sup> Considering that GO is an ultra-highly efficient quencher in fluorescence or

chemiluminescence body experiments, but also an electron transfer facilitator, and can be reduced and/or functionalized, the future of functionally hybridized GO is quite bright for its use in biosensing, since much interest is given to immobilization techniques for the fabrication of G-based electrochemical biosensors.<sup>139,160-162</sup> In a study, a multimodal probe based on bovine-serum-albumin-capped fluorine functionalized graphene quantum dots (BSA@FGQDs) was developed. This new fluorescent probe can monitor amyloid peptide monomers/oligomers with more sensitivity compared with previous ones.<sup>53</sup>

The characterizations of G and derivatives are routinely assessed by physical techniques such as microscopy (e.g. AFM, STM, SEM, TEM) and/or spectroscopy (e.g. Raman, XRD or Fourier-transform infrared [FTIR]) to unravel structure and molecular interactions. Their respective molecular behavior, including electro-oxidation degree, conductivity, molecular surface density, are usually assessed by voltammetry or chronoamperometry.

#### G and GO-Based Hybrid Nanocomposites: A Rational Boosting Interplay!

**Chemical Doping of G & GO.** The functionalization and the regulation of the electrocatalytic activity of G and derivatives can be achieved by chemicals.<sup>163,164</sup> Thereby, chemical doping of Gs can include the use of nitrogen (N), poly-L-lysine (PLL),



methylene blue (MB), polyamidoamine (PAMAM), polyallylamine (PAA), polydiacetylene (PDA), polyaniline (PA), 1-pyrenebutanoic acid, succinimidyl ester (PASE), polyethylene glycol (PEG).<sup>164-172</sup>

In an study, an N-doped GO electrochemical sensor prepared by thermally annealing GO and melamine mixture was able to simultaneously and sensitively detect ascorbic acid/vitamin C, dopamine and uric acid with a limit of detection (LOD) of 2.2  $\mu\text{M}$ , 0.25  $\mu\text{M}$ , and 45 nM, respectively. Besides, a reliable label-free electrochemical immunosensor based on G-MB-CS nanocomposite detected prostate specific antigen (PSA) from serum samples with a LOD as low as 13 pg/mL, which is better than current routine clinical devices (0-4 ng/mL).<sup>167</sup> Also, a first generation label-free sensor based on G-PAMAM-AuNPs was fabricated and tested for DNA hybridization sensing.<sup>173</sup> Compared to the vacuum techniques commonly used, the advanced PAMAM-SLG was immobilized covalently on mercaptopropionic acid monolayer containing a gold transducer. This sensor discriminated selectively and sensitively the complementary dsDNA (i.e. hybridized), non-complementary ssDNA (i.e. un-hybridized) and single nucleotide polymorphism (SNP) surfaces, with a LOD of 1 pM, which was 1000 times lower than PAMAM without G core. Further, a label-free electrochemical aptasensor based on G-polyaniline (G-PA) nanocomposites film was reported for detection of the neurotransmitter dopamine from human serum samples with a LOD of 1.98 pM.<sup>171</sup> Chemical modification of G with other elements can improve intrinsic properties, especially catalytic properties of G derivatives. The results showed that doping heteroatoms into the G lattice adapt the electronic and geometry features of the produced G by providing more active sites for stronger molecular adsorption.<sup>31</sup> Zhang et al have fabricated a new kind of doped G material through an economical and scalable thermal annealing approach which is useable in oxygen reduction reaction and lithium ion batteries.<sup>56</sup>

Besides, a performant, reliable and cost-effective sensor based a biocompatible hybrid nanocomposite coated onto SPE, namely GO-PASE/Tyr-Au/SPE, was constructed to detect tyrosinase (Tyr) with a LOD of 0.24 nM. Briefly, this nanocomposite was made by adsorption of GO sheets onto the bifunctional molecule 1-pyrenebutanoic acid succinimidyl ester (PASE) which covalently interacted with amines of Tyr-AuNPs (Tyr-Au).<sup>172</sup> Interestingly, a biocompatible film, assembled by combining GO and PLL, was used for adhesion, proliferation, drug-induced apoptosis (i.e. Nilotinib) and electrochemical impedance detection of cancer cells (i.e. leukemia K562 cells) with a LOD of 30 cells/mL.<sup>167</sup>

Further, rGO was electrochemically prepared on PA nanofibers-modified GCE to construct a nanocomposite-based sensor capable of detecting genes through non-covalent assembly of ssDNA to rGO-PA.<sup>174</sup> This rGO-PA-GCE was applied to a sequence-specific DNA of cauliflower mosaic

virus (CaMV35S) gene was with a LOD as low as 0.32 fmol/L. Also, a glucose sensor based on an electrochemical GOD-rGO-PLL-GCE was proposed with a linear range from 0.25 to 5 mmol.L<sup>-1</sup>.<sup>175</sup> In this case, GOD was immobilized on electrochemically rGO which was then adsorbed on PLL-modified GCE.

**Biological doping of G & GO.** During the last fifteen years, attempts have been made to dope G and GO with a number of biomolecules (e.g. polysaccharides such as chitosan [CS], proteins such as Hb, peptides such as peptide nucleic acid [PNA], lipids) in order to develop innovative compatible and always more and performant sensors. In general, the adsorption of these biomolecules on the surface of G or GO sheets leads to changes in membrane integrity of the biomolecule(s), which are then monitored electrically using an electrolyte-gated biomimetic membrane-G transistor.<sup>176-178</sup>

Thereby, a blood glucose biosensor based on G/AuNPs/CS nanocomposite film was constructed using a simple casting method which consisted in immobilizing GOD onto G-AuNPs-CS.<sup>179</sup> Recently reproducible electrocatalytic activity toward H<sub>2</sub>O<sub>2</sub> was demonstrated with a LOD of 180  $\mu\text{M}$ . These data are in line with a previous similar study, and comparing both studies it can be further concluded that AuNPs were useful to enhance the sensitivity of the amperometric response.<sup>180</sup> Another study described the development of a stable and performant G-CS-hemoglobin (Hb)-Ionic liquid (IL) GCE for the detection of nitromethane.<sup>181</sup> The presence of both G and IL not only dramatically facilitated the electron transfer of Hb, but also greatly enhanced the electrocatalytic activity toward nitromethane with a LOD of 60 nM.

A pioneered work reported a selective and sensitive GO-DNAzyme based biosensor for amplified fluorescence "turn-on" detection of Pb<sup>2+</sup> in river water samples with a LOD of 300 pM, which was lower than that previously reported for catalytic beacons. This biosensor was designed with a fluorescein amidite (FAM)-labeled DNAzyme-substrate hybrid that acted both as a molecular recognition module and signal reporter, GO acting as a super quencher. This biosensor has potential utility in medicine as it could also be applied to detect the presence of Pb<sup>2+</sup> levels in human blood samples to prevent or diagnose saturnism.<sup>182</sup>

Further, a stable rGO-hemin-GCE was used to detect Tyr with a LOD of 0.75 nM, which represents a sensitivity of 133 times higher than a bare GCE. Briefly, rGO was obtained by an original "green" and safe hydrothermal method and employed as a scaffold to adsorb the substrate hemin through  $\pi$ - $\pi$  interactions.<sup>29</sup>

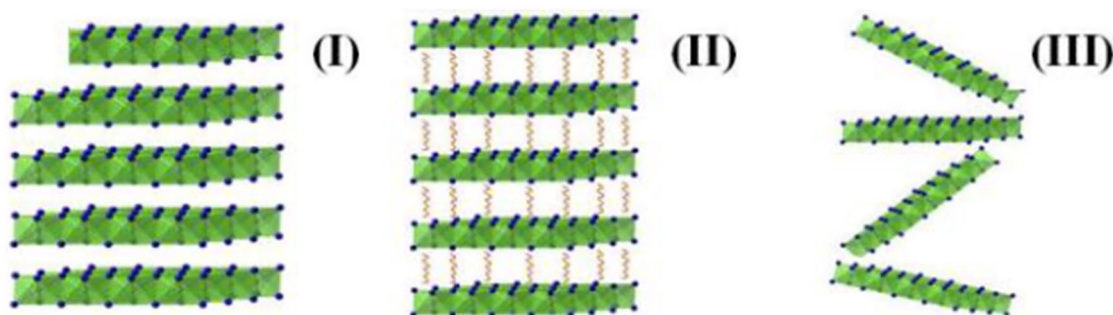
#### *Instruments and Devices Based on Functionalization/Doping of G and GO*

Nowadays, functionalized or doped G and G derivatives are among the most promising carbon nanomaterials for the

**Table 1.** Short meta-analysis of graphene-based biosensors for DNA detection.

SCAFFOLD	SUBSTRATE	MOLECULE	LOD (PM)	METHOD	REFERENCE
G	FET	DNA	3000	CVD	Guo et al <sup>145</sup>
rGO	PtNPs-FET	DNA	2400	LB/photochemical reduction of PtNPs	Yin et al <sup>146</sup>
GO	FRET	DNA	14 300	FAM-labeling	Alwarappan et al <sup>42</sup>
GO	CRET	DNA	5	Fluorophore-Exo III	Unnikrishnan et al <sup>178</sup>
rGO	AuNPs	DNA	0.005	HRP-CNS-AuNPs (TSA)	Dong et al <sup>183</sup>
G	AgNPs	DNA	72	Sandwich assay/AuNPs-catalyzed Ag deposition	Wang et al <sup>184</sup>
G	PANAM-AuNPs	DNA	1	Label free/dendrimer	Jayakumar et al <sup>173</sup>
G	PA-AuNPs	DNA	0.032	PA nanofibers modified GCE	Du et al <sup>174</sup>

Abbreviations: AuNPs, gold nanoparticles; CNS, carbon nanosphere; CVD, chemical vapor deposition; Exo III, exonuclease III; FAM, *fluorescein* amidite; GCE, glassy chemical electrode; HRP, horseradish peroxidase; LB, Langmuir Blodgett; LOD, limit of detection; PA, polyaniline; PtNPs, platinum nanoparticles; TSA, triple signal amplification.

**Figure 7.** Bulk layered materials (I), 2D material with a confined fluid and/or intercalated ions (II), and exfoliated (or nanosheet) 2D material (III).<sup>55</sup>

development of innovative biomolecular sensing platforms. From Table 1, it is noted that G (or derivatives)-Au nanocomposite provided the best LOD for DNA while FRET appears to be an obsolete method. Unfortunately, there is still a paucity of studies using Au (or Ag)-G-modified X doped diamond electrode (X could be Boron or other healthier minerals). Furthermore, to the best of our knowledge, comparative studies evaluating the performances of molecular sensing between G-diamond nanocomposites coupled (or not) to a diamond electrode with bare diamonds, are lacking. Yet, diamonds, likewise G, are considered as ideal and so the most promising semiconductors.

The 2D materials are a class of materials that are single- or few-atom thick crystals, that can be regarded as a new class of nanoscale materials, referred as “nanosheets”. They exhibit versatile properties due to their structural features that makes them interesting materials to be investigated. In 2D metal oxides, in-plane atoms are connected to each other by strong covalent bond, while the layers are held together by weak van der Waals interactions (Figure 7I). The individual layers are composed of metal-oxygen clusters and assembled in extended structures by sharing corners, edges and rarely faces (Figure 7II) and they can be further be exfoliated to their individual 2D units (Figure 7III).<sup>55</sup>

**G- and GO-based field-effect transistors (FETs).** G-based FETs (G-FETs), conducting channels for chemical and biosensing, were developed rapidly as an alternative for post-silicon electronics. Generally, molecular detection occurred by measuring changes in the FET sensor’s electrical signal upon molecular interaction (e.g. antibody-antigen binding).

Thereby, extremely sensitive and cost-effective G-based FET biosensors for label-free detection of DNA have been recently fabricated.<sup>158</sup> For such purpose, CVD-grown G layers were used to achieve FET devices’ mass production via conventional photolithographic patterning. Non-covalent functionalization of the G layer with 1-pyrenebutanoic acid succinimidyl ester (PASE) ensured high conductivity and sensitivity of the FET device (LOD of  $3 \times 10^{-9}$  M).

Also, large-sized G films fabricated by CVD were configured as FETs for real-time detection of glucose or glutamate.<sup>185</sup> The underlying mechanism relies on the conductance change of G-FET when molecular oxidation occurs by the specific redox enzyme (i.e. GOD or glutamic dehydrogenase) functionalized onto the G film.

Further, G-FETs driven by a reference-gate operating in buffer solution exhibited very good transport characteristics, allowing detection of pH value with high precision and sensitivity.<sup>186</sup>

Moreover, a label-free immunosensor based on an immunoglobulin E (IgE) aptamer-modified G-FET exhibited selective electrical detection of IgE protein (i.e. dissociation constant: 47 nM) and the drain current was found to be directly dependent on the IgE concentration.<sup>187</sup>

Interestingly, a G-liquid ion gated FET aptasensor, based on polypyrrole-converted nitrogen-doped few-layer G grown on Cu substrate, was fabricated by CVD for high sensitive detection (i.e. LOD of 100 fM) of vascular endothelial growth factor (VEGF), an angiogenesis biomarker.<sup>188</sup> This aptasensor also showed flexibility, high performance, excellent reusability, mechanical bendability, and durability.

Similarly, a more recent study reported a flexible CVD-grown G-FET used for highly sensitive glucose monitoring (LOD of 3.3–10.9 mM).<sup>189</sup> This sensor was functionalized with linker molecules to immobilize enzymes that induce the catalytic response of glucose, while polyethylene terephthalate was employed as the substrate material.

Importantly, a very high sensitivity and selectivity of G-FET biosensor was reported for protein detection (LOD: down to ~2 ng/mL or 13 pM) using vertically-oriented G sheets labeled with AuNP-antibody conjugates and directly grown on the sensor electrode using a plasma-enhanced CVD method.<sup>190</sup>

However, limiting aspects of using FET resides in the high and the difficulty of preparing reliable large-scale G films. Thus, other research groups have studied the possibility of developing biochemical sensors based on rGO-FETs because they rapidly, easily, and without the need for substrate and molecular labeling, detect biomolecules and their dynamics.<sup>160,191,192</sup> Thereby, a rGO-FET platform was proposed for increased sensitive glucose detection (LOD of 1.0  $\mu$ M). The modified electrode was prepared by one-step electrodeposition of the exfoliated rGO sheets onto an ionic liquid doped screen-printed electrode (IL-SPE).<sup>193</sup>

Besides, a simple but effective method to mass-produce rGO-based FETs allowing is being used. This is the case of few-layer rGO thin film fabricated on a Si (silicon)/SiO<sub>2</sub> wafer using the Langmuir-Blodgett (LB) method followed by thermal reduction.<sup>146</sup> Briefly, after photochemical reduction of platinum (Pt) NPs on rGO, the obtained PtNPs/rGO composite was employed as the conductive channel in a solution-gated FET, which was subsequently used for real-time and highly sensitive detection (LOD of 2.4 nM) of single-stranded DNA (ssDNA).

#### *G- and GO-based fluorescence resonance energy transfer (FRET).*

G- and GO-based FRET biosensors display unique real-time biomolecular adsorption (i.e. molecular binding interaction) and fluorescence nanoquenching activities.<sup>141,194</sup> Nevertheless, fine-tuning of the oxidation is a pre-requisite for G to avoid alterations in these activities which could lead to a broad range of sensitivity.<sup>195</sup>

Thereby, G-FRET biosensor was shown to homogeneously, selectively, rapidly (ca. 5 minutes) and sensitively detect (LOD of 0.8 nM) the lectin concanavalin A (ConA), a carbohydrate-binding protein.<sup>196</sup> For this purpose, maltose-grafted-aminopyrene was self-assembled on the surface of G by means of  $\pi$ -stacking interaction. Quenched fluorescence between G and pyrene rings in the presence of ConA was reverted (i.e. restoration of the fluorescence signal) by competitive binding of glucose that destroyed the  $\pi$ -stacking interaction. A similar approach has been reported to study peptide-protein interactions based on G-peptide complex.<sup>197</sup>

Interestingly, a versatile (i.e. fluorescence “on/off” switching strategy) and easily modifiable molecular beacon (MB)-like probe (e.g. specific oligonucleotide or antibody) can be used for rapid and sensitive (nM level) multiplex sensing of targets such as sequence-specific DNA, protein (e.g. thrombin), amino acid (e.g. cysteine), metal ions (e.g. Ag<sup>+</sup>, Hg<sup>2+</sup>) and small molecule compounds, based on the flexible and progressive self-assembled ssDNA-GO architecture.<sup>141</sup> Indeed, the interaction of GO and dye (as molecular beacon)-labeled DNA (i.e. ssDNA) lead to the quenching of the dye, but the presence of a target DNA or protein lead to the binding of dye-labeled DNA and target, releasing the DNA from GO, thereby restoring the dye fluorescence.<sup>140</sup> Importantly, the background fluorescence of the molecular beacon was significantly suppressed in the presence of GO, which increased signal-to-background ratio, thereby resulting in increased sensitivity. Furthermore, the large planar surface of GO allows simultaneous quenching of several DNA probes with different dyes, and so, it is suitable for production of a multiple biosensing platform with high sensitivity and selectivity.

Besides, GO-FRET was also employed for immunosensing of various molecules, including interleukin-5, enzymes (e.g. adenosine deaminase, matrix metalloproteinase 2 (MMP2), biothiols (e.g. glutathione, cysteine), proteins (e.g. thrombin, dopamine, DNA/DNA hybridization, miRNA and cancer cells. A highly stable GO-FRET sensor was developed by covalent assembly of fluorescein isothiocyanate-labeled peptide (Pep-FITC) onto the GO surface, for rapid (i.e. within 3 h), accurate, and highly sensitive detection in human serum samples (i.e. LOD of 2.5 ng/mL) of MMP-2, a cancer marker.<sup>36,198–204</sup>

Further, a GO-based photoinduced charge transfer (PCT) label-free near-infrared (NIR) fluorescent sensor was fabricated for selective, accurate and sensitive detection (LOD of 94 nM) of dopamine (DA).<sup>203</sup> In this study, the multiple non-covalent interactions between GO and DA and the ultrafast decay at the picosecond range of GO's NIR fluorescence resulted in effective self-assembly of DA molecules on the surface of GO and direct readout of the significant fluorescence quenching.

Also, a GO-FRET for sequence-specific recognition of double-stranded DNA (dsDNA) was developed based upon



the DNA hybridization between dye-labeled ssDNA and dsDNA.<sup>203</sup> The fluorescence of *fluorescein* amidite (FAM)-labeled ssDNA was quenched when it adsorbed on the surface of GO. Upon addition of the target dsDNA, a homopyrimidine/homopurine part of dsDNA (4424-4440, gp6) of the Simian virus 40 (SV40), hybridization occurred, which induced desorption of the dye-labeled DNA from the surface of GO, and turned on the fluorescence of dye. Under optimum conditions, the enhanced fluorescence intensity was sequence selective and proportional to the concentration of target dsDNA in the range 40.0 to 260 nM with a LOD of 14.3 nM.

Moreover, a simple, highly sensitive (i.e. LOD of 2.1 fM), and selective GO-FRET was performed for detection of simultaneous mi(micro)RNA labeled with different dyes, based on GO fluorescence quenching and isothermal strand-displacement polymerase reaction (ISDPR).<sup>204</sup> The strong interaction between ssDNA and GO led to the fluorescent ssDNA probe exhibiting minimal background fluorescence. Upon the recognition of specific target miRNA, ISDPR was triggered to produce numerous massive specific DNA-miRNA duplex helices, and a strong emission was observed due to the weak interaction between the DNA-miRNA duplex helix and GO.

Eventually, an efficient measurement of in situ cancer cells (CCRF-CEM, T lymphoblast cells) was performed using GO-FRET aptasensing microfluidic multiplex chip, which assessed cell-induced fluorescence recovery from dye-labeled aptamer/GO complex.<sup>205</sup> The fluorescence intensity measurement and image analyses demonstrated that this microfluidic biosensing method exhibited rapid and sensitive fluorescence responses to the quantities of the target cancer cells (i.e. LOD of 25 cells/mL, about ten times lower than conventional biosensors).

**G- and GO-based chemiluminescence resonance energy transfer (CRET).** G- and GO-based CRETs as photoelectrochemical sensing platforms have also raised tremendous interest.<sup>184,206</sup>

Thereby, an original immunosensing platform, using amplification techniques based on NIR- electrochemiluminescence (ECL) from CdTe/CdS core (small)/shell (thick) QDs, has been developed.<sup>184</sup> Briefly, AuNP-G nanosheet hybrids were prepared by a sonication-induced self-assembly and served as an effective matrix for primary antibody attachment. Then, the NIR-ECL nanoprobe (SiO<sub>2</sub>-QD-Ab2) involved covalent binding of a goat anti-human IgG antibody (used as a secondary antibody) on CdTe/CdS QDs-tagged silica nanospheres. After sandwich immunoreaction, functionalized silica nanosphere labels were captured onto the GCE surface. Integrating the dual amplification, by promoting the electron transfer rate of Au-G hybrids and increasing the QD loading of SiO<sub>2</sub>-QD-Ab2 labels, the NIR-ECL response from CdTe/CdS QDs was enhanced by 16.8 fold in comparison to the unamplified protocol. This enabled the ultrasensitive detection of human IgG with a LOD of 87 fg/mL.

Other advancements in the field include the development of a novel strategy for the enhancement of ECL based on the combination of G, CdS QDs and agarose.<sup>207</sup> Thereby, a G-CdS-QDs-agarose composite robust film was coated on GCE and conjugated to the binding linker, namely 3-aminopropyl-triethoxysilane. The resulting enhanced ECL was exploited to develop a biocompatible, extremely sensitive and stable label-free ECL immunosensor for the ultrasensitive and specific detection in maternal blood or amniotic fluid of  $\alpha$ -fetoprotein (AFP), a marker of human fetal abnormalities. Briefly, AFP-antibody was first immobilized onto the electrode through glutaric dialdehyde. The specific immunoreaction between AFP and its specific antibody resulted in decreased ECL intensity and increased in AFP concentration with a LOD of 0.2 fg/mL.

Besides, the bifunctionality of GO-CRET (i.e. high adsorption and effective emission quenching of organic dyes) is used for sensitive and selective molecular detection,<sup>208</sup> such as DNA sensing through peroxidic inhibition of a HRP-mimicking DNAzyme by GO.<sup>208</sup> Thereby, functionalized GO have been employed as functional matrices for chemiluminescent sensors to amplify the detection of DNA and aptamer-substrate complexes.<sup>209</sup> Briefly, fluorophore-labeled DNA strands acted as probes for 2 different DNA targets (i.e. thrombin and ATP) which were adsorbed onto GO, thereby leading to the quenching of luminescence of fluorophores. Desorption of probes from GO occurred by hybridizing with the target DNAs which led to the fluorescence of respective label. By coupling exonuclease III to the system, the recycling of target DNAs was demonstrated, which led to the amplified detection of DNA targets with a LOD of  $5 \times 10^{-12}$  M.

Eventually, rGO-CdS nanocomposite much improved the photovoltaic transfer efficiency of rGO-CRET, contributing to enhanced performance of photoelectrochemical immunoassays.<sup>210</sup> Amplified ECL of QDs generally employed rGO electrochemically for green biomolecular nanobiosensing.<sup>211-213</sup> Thereby, a sandwiched luminol ECL immunosensor using zinc oxide (ZnO) NPs, GOD labeled secondary antibody, and in situ generated H<sub>2</sub>O<sub>2</sub> as coreactant, was reported.<sup>213</sup> To construct the base of this immunosensor, hybrid architecture modified electrode of AuNPs and G was prepared by reduction of HAuCl<sub>4</sub> and GO with ascorbic acid. The enhanced sensitivity was obtained by the in-situ generation of H<sub>2</sub>O<sub>2</sub> by GOD and the catalysis of ZnONPs to the ECL reaction of luminol-H<sub>2</sub>O<sub>2</sub> system. This immunosensor served to detect the cancer biomarker, namely carcinoembryonic antigen (CEA), which was excellent with a LOD of 3.3 pg/mL. Moreover, QDs/rGO electrode, modified in presence of dissolved oxygen (O<sub>2</sub>) used as coreactant, showed drastic increase of ECL intensity, when compared to QDs, for choline (LOD of 8.8  $\mu$ M) and acetylcholine (LOD of 4.7  $\mu$ M) covalently cross-linked on this electrode with choline oxidase (ChO) and ChO-acetylcholinesterase, respectively.<sup>212</sup>

**G- and GO-based metallic surface plasmon resonance (SPR).** Owing to the high impermeability property of G to all gases and liquids, original labeled or unlabeled metallic SPR-G/SPR-GO has been developed for theranostic purposes. Thereby, a G or GO sheet was coated above a metallic thin film; metals include Au, silver (Ag), titanium ( $\text{TiO}_2$ ), platinum (Pt), cadmium (Cd), palladium (Pd), cobalt (Co), zinc (Zn), aluminium (Al).<sup>214-216</sup> These metallic SPR-Gs have been employed in biosensing to highly-accurate DNA strand sequencing, sensitive high-throughput assessment of multiple biomolecular interactions, quantitative and qualitative analysis of disease biomarkers.<sup>32,217,218</sup>

**Gs-based gold SPR.** Au-G and Au-GO SPR displayed excellent conductivity, stable and sensitive biomolecular adsorption due to  $\pi$ -stacking interactions.<sup>32,219</sup> Therefore, new enzyme-free amperometric Au-G SPR immunoassay platforms were created for rapid and sensitive detection of disease biomarkers (e.g. CEA, AFP), other proteins (e.g. heparin) and nucleic acid (e.g. DNA).<sup>217,219</sup> For instance, a simple and reliable amperometric immunosensor was fabricated by assembling methylene blue, AuNPs and CEA antibody layer-by-layer on a G-Nafion nanocomposite film-modified electrode for the detection of CEA with a LOD of 0.17 ng/mL.<sup>220</sup> Interestingly, Au-GO SPR, that could improve the sensing properties of Au-G SPR, was used for the reliable detection of AFP in human serum with a LOD of 1.0 pg/mL.<sup>219</sup> For this purpose, nanogold-functionalized magnetic GO nanosheets were used as immunosensing probes, and the fabrication of this reliable Au-GO SPR involved (i) the covalent immobilization of amino-functionalized magnetic beads on the surface of GO nanosheets; (ii) the adsorption of AuNPs on the amino groups; and (iii) the assembly of HRP-anti-AFP conjugates onto the surface of AuNPs, which were then magnetically attached onto the base electrode of the flow system. Also, several complex Au-G SPR nanocomposites were created for even higher sensitive detection of biomolecules (e.g. erythromycin, AFP, CEA) and chemicals (e.g.  $\text{H}_2\text{O}_2$ ). These nanocomposites include chitosan (CS)-PtNPs/AuNPs-G double nanocomposites; Au/Ag-G hybrid nanosheets; CS-ferrocene (Fc)/nano- $\text{TiO}_2$ /AuNPs-G and cadmium telluride (CdTe)-cadmium sulfide (CdS)/AuNPs-G nanohybrids.<sup>217,221-223</sup> Thereby, a novel label-free amperometric immunosensor based on CS-Fc/nano- $\text{TiO}_2$  complex film and AuNPs-G nanohybrid was constructed for enhanced sensitive detection of CEA with LOD of 3.4 pg/mL.<sup>223</sup> The bioanalytical procedure involved (i) the modification of CS-Fc +  $\text{TiO}_2$  composite membrane on a bare GCE; (ii) the formation of AuNPs-G nanohybrid on the CS-Fc- $\text{TiO}_2$  membrane by self-assembly; (iii) the immobilization of anti-CEA antibody employing the strong interactions between AuNPs-G and the amido groups of anti-CEA antibody.

**Gs-based silver SPR.** SLG deposited on a 60-nm thick Ag-film amplified the SPR biomolecular imaging signal more than 3 times, achieving higher sensitivity than the

conventional Au-film-based SPR imaging biosensor. Thereby, an electrochemical DNA sensor based on the assembly of G and DNA-conjugated AuNPs was fabricated using the silver enhancement strategy.<sup>224,225</sup> Briefly, the target DNA sequence and oligonucleotide probes-labeled AuNPs were able to hybridize in a sandwich assay format, following the AuNPs-catalyzed Ag deposition. Owing to the high DNA loading ability of G and the distinct signal amplification by AuNPs-catalyzed silver staining, the resulting biosensor exhibited a good analytical performance with a LOD of 72 pM, and enabled the discrimination of the complementary sequence from the single-base mismatch sequence. Further, GO sheet-mediated Ag enhancement exhibited rapid, highly sensitive and selective analysis of cells (e.g. microbes, biomolecules (e.g. platelet-derived growth factor (PDGF), thrombin, glucose and chemicals (e.g.  $\text{H}_2\text{O}_2$ )).<sup>148,227-228</sup> Thereby, a linear relationship between the stripping response and the logarithm of bacterial concentration was obtained using this electrochemical technique for concentrations ranging from  $1.8 \times 10^2$  to  $1.8 \times 10^8$  CFU/mL (slope of 15.28;  $r=0.995$ ).<sup>226</sup> Interestingly, the combination of with sol-gel technique enabled a pioneered work to report well-defined  $\text{SiO}_2$ -GO nanosheets decorated with AgNPs for the detection of  $\text{H}_2\text{O}_2$  and glucose in human serum.<sup>228,229</sup> Briefly, the  $\text{SiO}_2$ -GO nanocomposites were functionalized with  $\text{NH}_2$  group and employed as a support for direct (i.e. electrostatic adsorption) or indirect (i.e. pre-chemical reduction of Ag salts) loading of AgNPs. Finally, the glucose biosensor was constructed by immobilizing GOD onto AgNP/ $\text{SiO}_2$ -GO nanocomposite-modified GCE, which offered remarkable catalytic performance for  $\text{H}_2\text{O}_2$  reduction (LOD of  $4 \times 10^{-6}$  M) as well as fast amperometric response time.

**Gs-based platinum SPR.** Various methods of fabricating Pt-G hybrid nanocomposites (e.g. G/PtNPs/PA, Pt-G, G/PtAu/manganese dioxide ( $\text{MnO}_2$ ), GO-Pt-black, rGO-Pt for biological and chemical sensing enhancement were reported recently.<sup>230-234</sup>

Thereby, the Growth of coral-like PtAu- $\text{MnO}_2$  binary nanocomposites on free standing G paper was performed for flexible non-enzymatic glucose sensing.<sup>232</sup> Briefly, coral-like PtAu- $\text{MnO}_2$  nanocomposites were grown on the substrate through one-step template-free electrodeposition. This flexible electrode exhibited a unique set of structural and electrochemical properties such as better uniformity, larger active surface areas, and faster electron transfer in comparison with the control electrode prepared by tandem growth of  $\text{MnO}_2$  network and PtAu alloy. As a non-enzymatic amperometric biosensor, this reliable G/PtAu/ $\text{MnO}_2$  sensor showed great sensitivity and performance for glucose detection with a LOD of 0.02 mM. Besides, a biosensor platform composed of the water-soluble GO and Pt-black, an amorphously nanopatterned isoform of platinum metal, was prepared and tested for glucose sensing.<sup>233</sup> Briefly, Pt-black was electrodeposited onto GO. The effective surface area and electrocatalytic activity

toward  $\text{H}_2\text{O}_2$  oxidation as well as the sensitivity toward glucose oxidation of Pt-black/GO microelectrodes were significantly higher compared to that of Pt-black microelectrodes, thereby suggesting that Pt-black/GO nanocomposite facilitated an increase in electron transfer, and/or minimized mass transport limitations as compared to Pt-black alone. In comparison to the previous study, this glucose sensing platform seems to offer better overall results with a LOD of  $1\ \mu\text{M}$ .<sup>232,233</sup>

**Gs-based titanium SPR.** G-TiO<sub>2</sub> hybrid nanocomposites were developed for highly sensitive and rapid amperometric sensing of a number of molecules, including  $\text{H}_2\text{O}_2$ , ascorbic acid, dopamine, AFP, uric acid, glucose, organophosphates, trinitrotoluene (TNT).<sup>235,236</sup> Thereby, a simple, sensitive, selective and stable label-free platform based on TiO<sub>2</sub>-G, CS and AuNPs composite film modified GCE was developed for sensitive detection of AFP (LOD of  $0.03\ \text{ng/mL}$ ).<sup>237</sup> Briefly, the electrostatic adsorption of AuNPs (negatively charged) onto G-TiO<sub>2</sub>-CS composite film (positively charged) was followed by the immobilization of AFP antibody. Besides, a performant glucose biosensor with a linear amperometric response against a concentration of glucose ranging from 0 to  $8\ \text{mM}$  was reported based on the adsorption of GOD at a GO-TiO<sub>2</sub> composite electrode.<sup>236</sup> This hybrid nanocomposite was synthesized from a colloidal mixture of TiO<sub>2</sub> NPs and GO nanosheets by an aerosol assisted self-assembly.

**Gs-based cadmium SPR.** G-Cd nanocomposites are promising candidate for photoelectrochemical bioapplications because their heteronanostructure facilitates the spatial separation of charge carriers which results in enhanced photocurrent intensity.<sup>238,239</sup> They require only one-step synthesis in aqueous solution by LBL process.<sup>240</sup> Thereby, a Cds-G-TiO<sub>2</sub> biosensor, in which the neurotransmitter acetylcholinesterase (AChE) was immobilized on Cd-G nanocomposite, exhibited excellent performance for carbaryl (AChE inhibitor/pesticide) with a LOD of  $0.7\ \text{ng/mL}$ .<sup>238</sup> This biosensor provides a new promising tool for the analysis of enzyme inhibitors, albeit offering with slightly lower performance than G-TiO<sub>2</sub>.<sup>241</sup> Besides, an immunosensor based on Cd-GO nanoconjugates was made and employed for the detection of epithelial cell adhesion molecule (EpCAM) antigen, a tumor biomarker.<sup>239</sup> The nanoconjugates were fabricated by carboxylation of GO nanosheets to enable higher surface density of active sites for binding of streptavidin and amine-functionalized Cd-QDs via carbodiimide coupling chemistry. Subsequently, an immune reaction with biotinylated secondary antibodies occurred allowing sensitive detection with LOD as low as  $100\ \text{fg/mL}$  in PBS buffer and  $1\ \text{pg/mL}$  in serum samples, in addition to good selectivity, reproducibility, and long-storage stability.

**Gs-based palladium SPR.** There is still a paucity of reports about G-Pd sensors. Interestingly, a non-enzymatic electrochemical biosensor based on an electrode modified with PdNPs-functionalized G (i.e. PdNPs nafion-G) was fabricated for

glucose sensing.<sup>242</sup> PdNPs nafion-G was first assembled onto an electrode to chemically adsorb Pd<sup>2+</sup> ions, which were reduced by hydrazine hydrate to form PdNPs in situ. The resulting electrode showed a remarkably high electrochemical activity for electrocatalytic oxidation of glucose in alkaline medium and was applied to quantify glucose with a LOD of  $1\ \mu\text{M}$ . Further, PdNPs-CS-grafted G conjugates were prepared for glucose detection with LOD as low as  $0.2\ \mu\text{M}$ , which is about 5 times more sensitive than PdNPs nafion-G, through this summarized three-steps construction: (i) covalent functionalization of G with CS to improve its biocompatibility and hydrophilicity; (ii) dense decoration of CS-G with reduced PdNPs; (iii) covalent immobilization of GOD on GCE modified with the PdNPs-CS-G nanocomposite film.<sup>242,243</sup>

**Gs-based cobalt SPR.** G-Co based amperometric sensors also merit more attention. In some body experiments, Co-NPs-G nanocomposite-modified GCE prepared by electrodeposition were used for reliably detecting the essential aromatic amino-acid L-tryptophan (Trp) with a wide linear range and a LOD of  $0.01\ \mu\text{M}$ .<sup>244</sup> Besides, a high-quality sandwich-type electrochemical aptasensor based on CS-HCoPt bimetal hollow-rGO sheet was proposed to reliably detect the blood enzyme thrombin with a LOD of  $0.34\ \text{pM}$ .<sup>245</sup>

**Gs-based aluminium SPR.** Biosensors based on G-Al nanocomposite are rare. A proof-of-principle study described a robust multilayered G-Al nanopore platform prepared by electron-beam sculpting process for sensitive detection of DNA and DNA-protein complexes (i.e. DNA-RecA, an essential DNA binding repair protein).<sup>246</sup> The resulting G-Al<sub>2</sub>O<sub>3</sub> nanopores exhibited lower electrical noise than nanopores in pure G as well as high sensitivity to electrolyte pH at low KCl concentrations due to the high buffer capacity of Al<sub>2</sub>O<sub>3</sub>. Such nanopore integration with new G-based structures, such nanoribbons or nanogaps, could be an asset for theranostic applications including single-molecule DNA sequencing.

**Graphene-enhanced Raman scattering (GERS): The future is here!** Surface-enhanced Raman scattering (SERS) in general and on G in particular has been pioneered more than a decade ago by our team who wanted to test our patented technology called "Carbon-Fluor Raman Spectroscopy" (aka SpectroFluor™) on fluorinated (or not) carbon nanomaterials.<sup>247-249</sup> We showed that there is a synergistic enhanced Raman scattering effect of Fluor with G. Since then, others teams and studies including those of Ling et al<sup>250,251</sup> have extensively provide insights and prospects on GERS. The principles, mechanistic of application of this emerging method for biological (e.g. biomarkers of disease, DNA) and chemical sensing (e.g. 2,4,6-trinitrotoluene (TNT), food dyes) were relatively well reviewed this year.<sup>252</sup> Briefly, GERS effect was demonstrated when probes immobilized on G exhibited up to 17 times more Raman signals than those adsorbed on bare SiO<sub>2</sub>/Si substrates.<sup>250,251</sup> A chemical mechanism is attributed to the nature of GERS, and although



many parameters remain to be defined, it is stated that it is very important that the molecules are correctly oriented (HOMO-LUMO positions) and adsorbed well on the substrate surface so that charge-transfers and vibronic couplings can occur in a more reliable way.<sup>253</sup> Interestingly, GERS was able to detect 14 biomarkers associated with gastric cancer using GO-AuNPs nanocomposite, enabling the distinction of early and advanced gastric cancer patients from healthy individuals.<sup>254</sup>

These improved surface methods assessed with appropriate biomolecules, such as aptamer and inducers, caused ideal adhesion and detection. Further studies need to be conducted to predict the ideal structure in biosensing system and use synergistic combination of the 2 strategies in manufacturing engineered structures. Researchers should attend to more in-vivo experiments and analyze the structures. The study indicates that G family can attach to biomolecules in a controlled manner, and these additives significantly enhance or accelerate the adhesion and detection (response time).

### Conclusion and Perspectives

G is a name given to a crystalline monolayer form of carbon, tightly packed into a 2D honeycomb lattice. GO is the oxidative and water-soluble form of G, which has poor electrical conductivity due to its flaw in structure but because of its functional groups, it can easily link to biomolecules. Functional groups of GO can be reduced by hydrazine or different environment-friendly substances and form another G derivative named rGO. Although GO and rGO are derivatives of G and they are all used for enhancing cell growth, proliferation and differentiation, they exhibit different properties when used as a substrate for stem cells culture, such as higher protein loading potential of GO than G and also, biosensing. rGO has better electrical conductivity in comparison to GO, which makes it suitable for neural and muscular tissue applications whose functions are electric-based. GO is hydrophilic, so is preferred in solutions. It is concluded that hydrophilic surfaces such as GO detect and proliferate better, however by tuning the oxygen surface content of rGO (hydrophil) and suitable additives, it can be an efficient material for biosensing and regenerative medicine as well. Undeniably, there is still a tremendous interest for developing more performant, green, safe, compact, and portable point-of-care medical devices for on-site environmental and medical applications. In this regard, rational design and optimization of sensors based on graphene and derivative carbon nanomaterials are opening new horizons in the production of cost-effective biosensors. The upcoming construction of hybrid material systems, such as G-microcrystalline diamond, and resulting original device architectures shall provide a brighter future for next-generation optoelectronics platform systems like GERS.

### ORCID iD

Farid Mena  <https://orcid.org/0000-0002-0258-7322>

### REFERENCES

- Huebsch N, Mooney DJ. Inspiration and application in the evolution of biomaterials. *Nature*. 2009;462:426-432.
- Mena F, Abdelghani A, Mena B. Graphene nanomaterials as biocompatible and conductive scaffolds for stem cells: impact for tissue engineering and regenerative medicine. *J Tissue Eng Regen Med*. 2015;9:1321-1338.
- Vashist SK, Venkatesh AG, Mitsakakis K, et al. Nanotechnology-based biosensors and diagnostics: technology push versus industrial/healthcare requirements. *Bionanoscience*. 2012;2:115-126.
- Zhou Y, Ma M, He H, et al. Highly sensitive nitrite sensor based on AuNPs/RGO nanocomposites modified graphene electrochemical transistors. *Biosens Bioelectron*. 2019;146:111751.
- Yaragatti RM, Malode SJ, Shetti NP, et al. A novel sensor based on graphene oxide nanoparticles for the detection and analysis of an antihistamine drug. *Mater Today Proc*. 2019;18:780-787.
- Totaganti A, Malode SJ, Nayak DS, Shetti NP. Voltammetry and analytical applications of hydrochlorothiazide at graphene oxide modified glassy carbon electrode. *Mater Today Proc*. 2019;18:542-549.
- Boehm HP, Setton R, Stumpp E. Nomenclature and terminology of graphite intercalation compounds (IUPAC Recommendations 1994). *Pure Appl Chem*. 1994;66:1893-1901.
- Boehm H, Hofmann U. Surface properties of extremely thin graphite lamellae. In: *Proceedings of the Fifth Conference on Carbon*, Pennsylvania State University, University Park, PA, 1 January 1962. Pergamon.
- Chun S, Choi Y, Park W. All-graphene strain sensor on soft substrate. *Carbon*. 2017;116:753-759.
- Geim A, Novoselov K. The rise of graphene. *Nat Mater*. 2007;6:183-191.
- Abbott's IE. Graphene: exploring carbon flatland. *Phys Today*. 2007;60:35.
- Saito R, Fujita M, Dresselhaus G, Dresselhaus MS. Electronic structure of graphene tubules based on C<sub>60</sub>. *Phys Rev B Condens Matter*. 1992;46:1804-1811.
- Adam S, Hwang EH, Galitski VM, Sarma SD. A self-consistent theory for graphene transport. *Proc Natl Acad Sci*. 2007;104:18392-18397.
- Novoselov KS, Geim AK, Morozov SV, et al. Electric field effect in atomically thin carbon films. *Science*. 2004;306:666-669.
- Rutherford RB, Dudman RL. Ultra-thin flexible expanded graphite heating element. *Google patents*. 2003.
- Yue HY, Huang S, Chang J, et al. ZnO nanowire arrays on 3D hierarchical graphene foam: biomarker detection of Parkinson's disease. *ACS Nano*. 2014;8:1639-1646.
- Kuzmenko A, Van Heumen E, Carbone F, van der Marel D. Universal infrared conductance of graphite. *Phys Rev Lett*. 2008;100:117401.
- Kürüm U, Ekiz OÖ, Yaglioglu HG, et al. Electrochemically tunable ultrafast optical response of graphene oxide. *Appl Phys Lett*. 2011;98:141103.
- Chen S, Wu Q, Mishra C, et al. Thermal conductivity of isotopically modified graphene. *Nat Mater*. 2012;11:203-207.
- Heyrovská R. Atomic structures of graphene, benzene and methane with bond lengths as sums of the single, double and resonance bond radii of carbon. *arXiv Preprint arXiv:0804.4086*. 2008.
- Husale BS, Sahoo S, Radenovic A, Traversi F, Annibale P, Kis A. ssDNA binding reveals the atomic structure of graphene. *Langmuir*. 2010;26:18078-18082.
- Zheng Z, Zhao C, Lu S, et al. Microwave and optical saturable absorption in graphene. *Opt Express*. 2012;20:23201-23214.
- Wang et al. 3D hollow quasi-graphite capsules/polyaniline hybrid with a high performance for room-temperature ammonia gas sensors. *ACS Sens*. 2019;4:2343-2350.
- Geim AK. Graphene: status and prospects. *Science*. 2009;324:1530-1534.
- Bae S, Kim H, Lee Y, et al. Roll-to-roll production of 30-inch graphene films for transparent electrodes. *Nat Nanotechnol*. 2010;5:574-578.
- Park JS, Cho SM, Kim WJ, et al. Fabrication of graphene thin films based on layer-by-layer self-assembly of functionalized graphene nanosheets. *ACS Appl Mater Interfaces*. 2011;3:360-368.
- Shetti NP, Malode SJ, Malladi RS, Nargund SL, Shukla SS, Aminabhavi TM. Electrochemical detection and degradation of textile dye Congo red at graphene oxide modified electrode. *Microchem J*. 2019;146:387-392.
- Guo H-L, Wang XF, Qian QY, Wang FB, Xia XH. A green approach to the synthesis of graphene nanosheets. *ACS Nano*. 2009;3:2653-2659.
- Lu L, Seenivasan R, Wang Y.-C., Yu J.-H, Gunasekaran S. An electrochemical immunosensor for rapid and sensitive detection of mycotoxins fumonisin B1 and deoxynivalenol. *Electrochim Acta*. 2016;213:89-97.
- Riedl C, Coletti C, Iwasaki T, Zakharov AA, Starke U. Quasi-free-standing epitaxial graphene on SiC obtained by hydrogen intercalation. *Phys Rev Lett*. 2009;103:246804.
- Sutter P. How silicon leaves the scene. *Nat Mater*. 2009;8:171-172.
- Song B, Li D, Qi W, Elstner M, Fan C, Fang H. Graphene on Au (111): a highly conductive material with excellent adsorption properties for high-resolution bio/nanodetection and identification. *ChemPhysChem*. 2010;11:585-589.
- Mena F, Vashist SK, Abdelghani A, Mena B. Graphene-based nanosystems for the detection of proteinic biomarkers of disease: implication in translational

- medicine. In: Eshaghian-Wilner MM (ed.) *Wireless Computing in Medicine*. 2016:377-399.
34. Shen H, Zhang L, Liu M, Zhang Z. Biomedical applications of graphene. *Theranostics*. 2012;2:283-294.
  35. Sanchez VC, Jachak A, Hurt RH, Kane AB. Biological interactions of graphene-family nanomaterials: an interdisciplinary review. *Chem Res Toxicol*. 2012;25: 15-34.
  36. Mena F. When pharma meets nano or the emerging era of nanopharmaceuticals. *Pharmaceut Anal Acta*. 2013;4:223.
  37. Shenderova O, Zhirnov V, Brenner D. Carbon nanostructures. *Crit Rev Solid State Mater Sci*. 2002;27:227-356.
  38. Braga SF, Coluci VR, Legoas SB, Giro R, Galvão DS, Baughman RH. Structure and dynamics of carbon nanoscrolls. *Nano Lett*. 2004;4:881-884.
  39. Dresselhaus MS, Araujo PT. *Perspectives on the 2010 Nobel Prize in Physics for Graphene*. ACS Publications; 2010.
  40. Rao CN, Sood AK, Voggu R, Subrahmanyam KS. Some novel attributes of graphene. *J Phys Chem Lett*. 2010;1:572-580.
  41. Zheng D, Vashist SK, Al-Rubeaan K, Luong JH, Sheu FS. Mediatorless amperometric glucose biosensing using 3-aminopropyltriethoxysilane-functionalized graphene. *Talanta*. 2012;99:22-28.
  42. Alwarappan S, Erdem A, Liu C, Li CZ. Probing the electrochemical properties of graphene nanosheets for biosensing applications. *J Phys Chem C*. 2009;113: 8853-8857.
  43. Yavari F, Koratkar N. Graphene-based chemical sensors. *J Phys Chem Lett*. 2012;3:1746-1753.
  44. Shan C, Yang H, Song J, Han D, Ivaska A, Niu L. Direct electrochemistry of glucose oxidase and biosensing for glucose based on graphene. *Anal Chem*. 2009;81:2378-2382.
  45. Lv W, Jin FM, Guo Q, Yang QH, Kang F. DNA-dispersed graphene/NiO hybrid materials for highly sensitive non-enzymatic glucose sensor. *Electrochim Acta*. 2012;73:129-135.
  46. Mazhabi RM, Ge L, Jiang H, Wang X. A label-free aptamer-based cytosensor for specific cervical cancer HeLa cell recognition through a g-C<sub>3</sub>N<sub>4</sub>-AgI/ITO photoelectrode†. *J Mater Chem B*. 2018;6:5039-5049.
  47. Liu M, Liu R, Chen W. Graphene wrapped Cu<sub>2</sub>O nanocubes: non-enzymatic electrochemical sensors for the detection of glucose and hydrogen peroxide with enhanced stability. *Biosens Bioelectron*. 2013;45:206-212.
  48. Yang F, Fu de L, Long J, Ni QX. Magnetic lymphatic targeting drug delivery system using carbon nanotubes. *Med Hypotheses*. 2008;70:765-767.
  49. Srivastava RK, Pant AB, Kashyap MP, et al. Multi-walled carbon nanotubes induce oxidative stress and apoptosis in human lung cancer cell line-A549. *Nanotoxicology*. 2011;5:195-207.
  50. Aslam S, Sagar RU, Liu Y, et al. Graphene decorated polymeric flexible materials for lightweight high areal energy lithium-ion batteries. *Appl Mater Today*. 2019;17:123-129.
  51. Tian L, Mezziani MJ, Lu F, et al. Graphene oxides for homogeneous dispersion of carbon nanotubes. *ACS Appl Mater Interfaces*. 2010;2:3217-3222.
  52. Kim J, Tung VC, Huang J. Water processable graphene oxide: single walled carbon nanotube composite as anode modifier for polymer solar cells. *Adv Energy Mater*. 2011;1:1052-1057.
  53. Li J, Kuang D, Feng Y, et al. Green synthesis of silver nanoparticles-graphene oxide nanocomposite and its application in electrochemical sensing of tryptophan. *Biosens Bioelectron*. 2013;42:198-206.
  54. Zhu X, Xu J, Duan X, et al. Multi-walled carbon nanotubes-amine reduced graphene oxide modified glassy carbon electrode as the voltammetric sensor for sensitive electrochemical determination of rutin. *Int J Electrochem Sci*. 2015;10:9192-9204.
  55. Zhang Q, Yang S, Zhang J, et al. Fabrication of an electrochemical platform based on the self-assembly of graphene oxide-multiwall carbon nanotube nanocomposite and horseradish peroxidase: direct electrochemistry and electrocatalysis. *Nanotechnology*. 2011;22:494010.
  56. Niyogi S, Bekyarova E, Itkis ME, McWilliams JL, Hamon MA, Haddon RC. Solution properties of graphite and graphene. *J Am Chem Soc*. 2006;128: 7720-7721.
  57. Eswaraiiah V, Aravind SSJ, Ramaprabhu S. Top down method for synthesis of highly conducting graphene by exfoliation of graphite oxide using focused solar radiation. *J Mater Chem*. 2011;21:6800-6803.
  58. Chen JH, Jang C, Adam S, Fuhrer MS, Williams ED, Ishigami M. Charged-impurity scattering in graphene. *Nat Phys*. 2008;4:377-381.
  59. Carlsson JM. Buckle or break. *Nat Mater*. 2007;6:801-802.
  60. Bolmatov D. Thermodynamic properties of tunneling quasiparticles in graphene-based structures. *Phys C Supercond*. 2011;471:1651-1654.
  61. Zan R, Ramasse QM, Bangert U, Novoselov KS. Graphene reknits its holes. *Nano Lett*. 2012;12:3936-3940.
  62. Meyer JC, Geim AK, Katsnelson MI, Novoselov KS, Booth TJ, Roth S. The structure of suspended graphene sheets. *Nature*. 2007;446:60-63.
  63. Kasuya D, Yudasaka M, Takahashi K, Kokai F, Iijima S. Selective production of single-wall carbon nanohorn aggregates and their formation mechanism. *J Phys Chem B*. 2002;106:4947-4951.
  64. Ishigami M, Chen JH, Cullen WG, Fuhrer MS, Williams ED. Atomic structure of graphene on SiO<sub>2</sub>. *Nano Lett*. 2007;7:1643-1648.
  65. Stolyarova E, Rim KT, Ryu S, et al. High-resolution scanning tunneling microscopy imaging of mesoscopic graphene sheets on an insulating surface. *Proc Natl Acad Sci*. 2007;104:9209-9212.
  66. Sakamoto J, van Heijst J, Lukin O, Schlüter AD. Two-dimensional polymers: just a dream of synthetic chemists? *Angew Chem Int Ed Engl*. 2009;48:1030-1069.
  67. Semenoff GW. Condensed-matter simulation of a three-dimensional anomaly. *Phys Rev Lett*. 1984;53:2449.
  68. Hernández-Ortiz S, Murguía G, Raya A. Hard and soft supersymmetry breaking for 'graphino' in uniform magnetic fields. *J Phys Condens Matter*. 2011;24:015304.
  69. Wallace PR. The band theory of graphite. *Phys Rev*. 1947;71:622.
  70. Avouris P, Chen Z, Perebeinos V. Carbon-based electronics. *Nat Nanotechnol*. 2007;2:605-615.
  71. Charlier JC, Eklund PC, Zhu J, Ferrari AC. Electron and phonon properties of graphene: their relationship with carbon nanotubes. In: Jorio A, Dresselhaus G, Dresselhaus MS (eds) *Carbon Nanotubes*. Springer; 2007:673-709.
  72. Xia J, Chen F, Li J, Tao N. Measurement of the quantum capacitance of graphene. *Nat Nanotechnol*. 2009;4:505-509.
  73. Chen F, Xia J, Ferry DK, Tao N. Dielectric screening enhanced performance in graphene FET. *Nano Lett*. 2009;9:2571-2574.
  74. Min H, Sahu B, Banerjee SK, MacDonald AH. Ab initio theory of gate induced gaps in graphene bilayers. *Phys Rev B*. 2007;75:155115.
  75. Barlas Y, Côté R, Lambert J, MacDonald AH. Anomalous exciton condensation in graphene bilayers. *Phys Rev Lett*. 2010;104:096802.
  76. Brown L, Hovden R, Huang P, Wojcik M, Muller DA, Park J. Twinning and twisting of tri- and bilayer graphene. *Nano Lett*. 2012;12:1609-1615.
  77. Nair RR, Blake P, Grigorenko AN, et al. Fine structure constant defines visual transparency of graphene. *Science*. 2008;320:1308-1308.
  78. Liu J, Wright AR, Zhang C, Ma Z. Strong terahertz conductance of graphene nanoribbons under a magnetic field. *Appl Phys Lett*. 2008;93:041106.
  79. Bao Q, Zhang H, Wang Y, et al. Atomic-layer graphene as a saturable absorber for ultrafast pulsed lasers. *Adv Funct Mater*. 2009;19:3077-3083.
  80. Zhang H, Virally S, Bao Q, et al. Z-scan measurement of the nonlinear refractive index of graphene. *Opt Lett*. 2012;37:1856-1858.
  81. Sreekanth KV, Zeng S, Shang J, Yong KT, Yu T. Excitation of surface electromagnetic waves in a graphene-based Bragg grating. *Sci Rep*. 2012;2:737.
  82. Mishra A, Basu S, Shetti NP, Reddy KR, Aminabhavi TM. Photocatalysis of graphene and carbon nitride-based functional carbon quantum dots. In: Thomas S, Pasquini D, Leu S-Y, Gopakumar DA (eds) *Nanoscale Materials in Water Purification*. Elsevier; 2019:759-781.
  83. Lee C, Wei X, Kysar JW, Hone J. Measurement of the elastic properties and intrinsic strength of monolayer graphene. *Science*. 2008;321:385-388.
  84. Bordag M, Fialkovsky IV, Gitman DM, Vassilevich DV. Casimir interaction between a perfect conductor and graphene described by the Dirac model. *Phys Rev B*. 2009;80:245406.
  85. Fialkovsky IV, Marachevsky VN, Vassilevich DV. Finite-temperature Casimir effect for graphene. *Phys Rev B*. 2011;84:035446.
  86. Dobson JF, White A, Rubio A. Asymptotics of the dispersion interaction: analytic benchmarks for van der Waals energy functionals. *Phys Rev Lett*. 2006;96:073201.
  87. Balandin AA, Ghosh S, Bao W, et al. Superior thermal conductivity of single-layer graphene. *Nano Lett*. 2008;8:902-907.
  88. Mingo N, Broido D. Carbon nanotube ballistic thermal conductance and its limits. *Phys Rev Lett*. 2005;95:096105.
  89. Dakshayini BS, Reddy KR, Mishra A, et al. Role of conducting polymer and metal oxide-based hybrids for applications in amperometric sensors and biosensors. *Microchem J*. 2019;147:7-24.
  90. Devarushi US, Shetti NP, Malode SJ, Tuwar SM. Electro oxidation and analytical applications of nimesulide at graphene oxide and reduced graphene oxide modified carbon paste electrode. *Mater Today Proc*. 2019;18:751-758.
  91. Justino CI, Gomes AR, Freitas AC, Duarte AC, Rocha-Santos TA. Graphene based sensors and biosensors. *TrAC Trends Anal Chem*. 2017;91:53-66.
  92. Shetti NP, Bukkitgar SD, Reddy KR, Reddy CV, Aminabhavi TM. ZnO-based nanostructured electrodes for electrochemical sensors and biosensors in biomedical applications. *Biosens Bioelectron*. 2019;141:111417.
  93. Zeng G, Xing Y, Gao J, Wang Z, Zhang X. Unconventional layer-by-layer assembly of graphene multilayer films for enzyme-based glucose and maltose biosensing. *Langmuir*. 2010;26:15022-15026.
  94. Gu H, Yu Y, Liu X, Ni B, Zhou T, Shi G. Layer-by-layer self-assembly of functionalized graphene nanoplates for glucose sensing in vivo integrated with on-line microdialysis system. *Biosens Bioelectron*. 2012;32:118-126.
  95. Chang H, Wu X, Wu C, Chen Y, Jiang H, Wang X. Catalytic oxidation and determination of β-NADH using self-assembly hybrid of gold nanoparticles and graphene. *Analyst*. 2011;136:2735-2740.
  96. Liu Y, Liu Y, Feng H, et al. Layer-by-layer assembly of chemical reduced graphene and carbon nanotubes for sensitive electrochemical immunoassay. *Biosens Bioelectron*. 2012;35:63-68.
  97. Gútes A, Carraro C, Maboudian R. Single-layer CVD-grown graphene decorated with metal nanoparticles as a promising biosensing platform. *Biosens Bioelectron*. 2012;33:56-59.

98. Li X, Cai W, An J, et al. Large-area synthesis of high-quality and uniform graphene films on copper foils. *Science*. 2009;324:1312-1314.
99. Kosynkin DV, Higginbotham AL, Sinitskii A, et al. Longitudinal unzipping of carbon nanotubes to form graphene nanoribbons. *Nature*. 2009;458:872-876.
100. Choucair M, Thordarson P, Stride JA. Gram-scale production of graphene based on solvothermal synthesis and sonication. *Nat Nanotechnol*. 2009;4:30-33.
101. Kumar S, Bukhtigar SD, Singh S, et al. Electrochemical sensors and biosensors based on graphene functionalized with metal oxide nanostructures for healthcare applications. *ChemistrySelect*. 2019;4:5322-5337.
102. Mahmood N, De Castro IA, Pramoda K, Khoshmanesh K, Bhargava SK, Kalantar-Zadeh K. Atomically thin two-dimensional metal oxide nanosheets and their heterostructures for energy storage. *Energy Storage Mater*. 2019;16: 455-480.
103. Chakrabarti A, Lu J, Skrabutenas JC, et al. Conversion of carbon dioxide to few-layer graphene. *J Mater Chem*. 2011;21:9491-9493.
104. Zhou SY, Gweon GH, Graf J, et al. First direct observation of Dirac fermions in graphite. *Nat Phys*. 2006;2:595-599.
105. Ohta T, Bostwick A, McChesney JL, Seyller T, Horn K, Rotenberg E. Interlayer interaction and electronic screening in multilayer graphene investigated with angle-resolved photoemission spectroscopy. *Phys Rev Lett*. 2007;98:206802.
106. Shen T, Gu JJ, Xu M, et al. Observation of quantum-Hall effect in gated epitaxial graphene grown on SiC (0001). *Appl Phys Lett*. 2009;95:172105.
107. Lara-Avila S, Kalaboukhov A, Paolillo S, et al. SiC graphene suitable for quantum hall resistance metrology. *arXiv Preprint arXiv:0909.1193*. 2009.
108. Bostwick A, Ohta T, McChesney JL, et al. Symmetry breaking in few layer graphene films. *NJ Phys*. 2007;9:385.
109. Hass J, Varchon F, Millan-Otoya JE, et al. Why multilayer graphene on 4 H-SiC (0001) behaves like a single sheet of graphene. *Phys Rev Lett*. 2008;100: 125504.
110. Pletikosić I, Kralj M, Pervan P, et al. Dirac cones and minigaps for graphene on Ir (111). *Phys Rev Lett*. 2009;102:056808.
111. Yuan Y, Wang Y, Wang H, Hou S. Gold nanoparticles decorated on single layer graphene applied for electrochemical ultrasensitive glucose biosensor. *J Electroanal Chem*. 2019;855:113495.
112. Amini S, Garay J, Liu G, Balandin AA, Abbaschian R. Growth of large-area graphene films from metal-carbon melts. *J Appl Phys*. 2010;108:094321.
113. Wassei JK, Mecklenburg M, Torres JA, et al. Chemical vapor deposition of graphene on copper from methane, ethane and propane: evidence for bilayer selectivity. *Small*. 2012;8:1415-1422.
114. Lenski DR, Fuhrer MS. Raman and optical characterization of multilayer turbostratic graphene grown via chemical vapor deposition. *J Appl Phys*. 2011;110: 013720.
115. Kim KS, Zhao Y, Jang H, et al. Large-scale pattern growth of graphene films for stretchable transparent electrodes. *Nature*. 2009;457:706-710.
116. Kosynkin DV, Higginbotham AL, Sinitskii A, et al. Longitudinal unzipping of carbon nanotubes to form graphene nanoribbons. *Nature*. 2009;458:872-876.
117. Jiao L, Zhang L, Wang X, Diankov G, Dai H. Narrow graphene nanoribbons from carbon nanotubes. *Nature*. 2009;458:877-880.
118. Neto AC, Guinea F, Peres NM, Novoselov KS, Geim AK. The electronic properties of graphene. *Rev Mod Phys*. 2009;81:109-162.
119. Barone V, Hod O, Scuseria GE. Electronic structure and stability of semiconducting graphene nanoribbons. *Nano Lett*. 2006;6:2748-2754.
120. Mohanty N, Moore D, Xu Z, et al. Nanotomy-based production of transferable and dispersible graphene nanostructures of controlled shape and size. *Nat Commun*. 2012;3:1-8.
121. Wang ZF, Shi QW, Li Q, et al. Z-shaped graphene nanoribbon quantum dot device. *Appl Phys Lett*. 2007;91:053109.
122. Shen J, Zhu Y, Yang X, Li C. Graphene quantum dots: emergent nanolights for bioimaging, sensors, catalysis and photovoltaic devices. *Chem Commun*. 2012;48:3686-3699.
123. Yousaf M, Ahmad M, Bhatti IA, et al. In vivo and in vitro monitoring of amyloid aggregation via BSA@FGQDs multimodal probe. *ACS Sens*. 2018;4:200-210.
124. Alzari V, Nuvoli D, Scognamiglio S, et al. Graphene-containing thermoresponsive nanocomposite hydrogels of poly (N-isopropylacrylamide) prepared by frontal polymerization. *J Mater Chem*. 2011;21:8727-8733.
125. Nuvoli D, Valentini L, Alzari V, et al. High concentration few-layer graphene sheets obtained by liquid phase exfoliation of graphite in ionic liquid. *J Mater Chem*. 2011;21:3428-3431.
126. William S, Hummers J, Offeman RE. Preparation of graphitic oxide. *J Am Chem Soc*. 1958;80:1339-1339.
127. Marcano DC, Kosynkin DV, Berlin JM, et al. Improved synthesis of graphene oxide. *ACS Nano*. 2010;4:4806-4814.
128. Chiu PL, Mastrogiovanni DD, Wei D, et al. Microwave-and nitronium ion-enabled rapid and direct production of highly conductive low-oxygen graphene. *J Am Chem Soc*. 2012;134:5850-5856.
129. Whitby RL, Korobeinyk A, Glevatska KV. Morphological changes and covalent reactivity assessment of single-layer graphene oxides under carboxylic group-targeted chemistry. *Carbon*. 2011;49:722-725.
130. Artiles MS, Rout CS, Fisher TS. Graphene-based hybrid materials and devices for biosensing. *Adv Drug Deliv Rev*. 2011;63:1352-1360.
131. Wang X, Wang J, Cheng H, Yu P, Ye J, Mao L. Graphene as a spacer to layer-by-layer assemble electrochemically functionalized nanostructures for molecular bioelectronic devices. *Langmuir*. 2011;27:11180-11186.
132. Wujcik EK, Monty CN. Nanotechnology for implantable sensors: carbon nanotubes and graphene in medicine. *Wiley Interdiscip Rev Nanomed Nanobiotechnol*. 2013;5:233-249.
133. Jian X, Wang H, Rao G, et al. Self-tunable ultrathin carbon nanocups as the electrode material of sodium-ion batteries with unprecedented capacity and stability. *Chem Eng J*. 2019;364:578-588.
134. Li Q, Mahmood N, Zhu J, Hou Y, Sun S. Graphene and its composites with nanoparticles for electrochemical energy applications. *Nano Today*. 2014;9: 668-683.
135. Srivastava RK, Srivastava S, Narayanan TN, et al. Functionalized multilayered graphene platform for urea sensor. *ACS Nano*. 2012;6:168-175.
136. Shetti NP, Malode SJ, Nayak DS, et al. A novel biosensor based on graphene oxide-nanoclay hybrid electrode for the detection of Theophylline for healthcare applications. *Microchem J*. 2019;149:103985.
137. Kuila T, Bose S, Khanra P, Mishra AK, Kim NH, Lee JH. Recent advances in graphene-based biosensors. *Biosens Bioelectron*. 2011;26:4637-4648.
138. Wang Y, Li Z, Wang J, Li J, Lin Y. Graphene and graphene oxide: biofunctionalization and applications in biotechnology. *Trends Biotechnol*. 2011;29:205-212.
139. Morales-Narváez E, Merkoçi A. Graphene oxide: graphene oxide as an optical biosensing platform (Adv. Mater. 25/2012). *Adv Mater*. 2012;24:3289-3289.
140. Lu CH, Yang HH, Zhu CL, Chen X, Chen GN. A graphene platform for sensing biomolecules. *Angew Chem Int Ed Engl*. 2009;48:4785-4787.
141. Zhang M, Yin BC, Tan W, Ye BC. A versatile graphene-based fluorescence "on/off" switch for multiplex detection of various targets. *Biosens Bioelectron*. 2011;26: 3260-3265.
142. Ge S, Yan M, Lu J, et al. Electrochemical biosensor based on graphene oxide-Au nanoclusters composites for l-cysteine analysis. *Biosens Bioelectron*. 2012;31: 49-54.
143. Huang KJ, Niu DJ, Sun JY, et al. Novel electrochemical sensor based on functionalized graphene for simultaneous determination of adenine and guanine in DNA. *Colloids Surf B Biointerfaces*. 2011;82:543-549.
144. Akhavan O, Ghaderi E, Rahighi R. Toward single-DNA electrochemical biosensing by graphene nanowalls. *ACS Nano*. 2012;6:2904-2916.
145. Guo SR, Lin J, Penchev M, et al. Label free DNA detection using large area graphene based field effect transistor biosensors. *J Nanosci Nanotechnol*. 2011;11: 5258-5263.
146. Yin Z, He Q, Huang X, et al. Real-time DNA detection using Pt nanoparticle-decorated reduced graphene oxide field-effect transistors. *Nanoscale*. 2012;4: 293-297.
147. James Yang C. Graphene oxide-protected DNA probes for multiplex microRNA analysis in complex biological samples based on a cyclic enzymatic amplification method. *Chem Commun*. 2012;48:194-196.
148. Wang Y, Yuan R, Chai Y, Yuan Y, Bai L. In situ enzymatic silver enhancement based on functionalized graphene oxide and layer-by-layer assembled gold nanoparticles for ultrasensitive detection of thrombin. *Biosens Bioelectron*. 2012; 38:50-54.
149. Sun CL, Lee HH, Yang JM, Wu CC. The simultaneous electrochemical detection of ascorbic acid, dopamine, and uric acid using graphene/size-selected Pt nanocomposites. *Biosens Bioelectron*. 2011;26:3450-3455.
150. Feng T, Feng D, Shi W, Li X, Ma H. A graphene oxide-peptide fluorescence sensor for proteolytically active prostate-specific antigen. *Mol Biosyst*. 2012;8: 1441-1445.
151. Song E, Cheng D, Song Y, Jiang M, Yu J, Wang Y. A graphene oxide-based FRET sensor for rapid and sensitive detection of matrix metalloproteinase 2 in human serum sample. *Biosens Bioelectron*. 2013;47:445-450.
152. Zheng D, Vashist SK, Dykas MM, et al. Graphene versus multi-walled carbon nanotubes for electrochemical glucose biosensing. *Materials*. 2013;6:1011-1027.
153. Liu M, Zhao H, Chen S, Yu H, Zhang Y, Quan X. Label-free fluorescent detection of Cu (II) ions based on DNA cleavage-dependent graphene-quenched DNazymes. *Chem Commun*. 2011;47:7749-7751.
154. He Y, Wang ZG, Tang HW, Pang DW. Low background signal platform for the detection of ATP: when a molecular aptamer beacon meets graphene oxide. *Biosens Bioelectron*. 2011;29:76-81.
155. Zhang JR, Huang WT, Xie WY, Wen T, Luo HQ, Li NB. Highly sensitive, selective, and rapid fluorescence Hg<sup>2+</sup> sensor based on DNA duplexes of poly (dT) and graphene oxide. *Analyst*. 2012;137:3300-3305.
156. Chikkaveeriah BV, Soldà A, Choudhary D, Maran F, Rusling JF. Ultrasensitive nanostructured immunosensor for stem and carcinoma cell pluripotency gate-keeper protein NANOG. *Nanomedicine*. 2012;7:957-965.
157. Mannoor MS, Tao H, Clayton JD, et al. Graphene-based wireless bacteria detection on tooth enamel. *Nat Commun*. 2012;3:763.
158. Wan Y, Lin Z, Zhang D, Wang Y, Hou B. Impedimetric immunosensor doped with reduced graphene sheets fabricated by controllable electrodeposition for the non-labelled detection of bacteria. *Biosens Bioelectron*. 2011;26:1959-1964.



159. Nalla V, Polavarapu L, Manga KK, et al. Transient photoconductivity and femtosecond nonlinear optical properties of a conjugated polymer-graphene oxide composite. *Nanotechnology*. 2010;21:415203.
160. He Q, Sudibya HG, Yin Z, et al. Centimeter-long and large-scale micropatterns of reduced graphene oxide films: fabrication and sensing applications. *ACS Nano*. 2010;4:3201-3208.
161. Putzbach W, Ronkainen NJ. Immobilization techniques in the fabrication of nano-material-based electrochemical biosensors: a review. *Sensors*. 2013;13: 4811-4840.
162. Shetti NP, Nayak DS, Malode SJ, et al. Electrooxidation and determination of flufenamic acid at graphene oxide modified carbon electrode. *Surf Interfaces*. 2017;9:107-113.
163. Wang Y, Shao Y, Matson DW, Li J, Lin Y. Nitrogen-doped graphene and its application in electrochemical biosensing. *ACS Nano*. 2010;4:1790-1798.
164. Zhang X, Huang PJ, Servos MR, Liu J. Effects of polyethylene glycol on DNA adsorption and hybridization on gold nanoparticles and graphene oxide. *Langmuir*. 2012;28:14330-14337.
165. Sheng ZH, Zheng XQ, Xu JY, Bao WJ, Wang FB, Xia XH. Electrochemical sensor based on nitrogen doped graphene: simultaneous determination of ascorbic acid, dopamine and uric acid. *Biosens Bioelectron*. 2012;34:125-131.
166. Shan C, Yang H, Han D, Zhang Q, Ivaska A, Niu L. Water-soluble graphene covalently functionalized by biocompatible poly-L-lysine. *Langmuir*. 2009;25: 12030-12033.
167. Zhang D, Zhang Y, Zheng L, Zhan Y, He L. Graphene oxide/poly-l-lysine assembled layer for adhesion and electrochemical impedance detection of leukemia K562 cancer cells. *Biosens Bioelectron*. 2013;42:112-118.
168. Mao K, Wu D, Li Y, et al. Label-free electrochemical immunosensor based on graphene/methylene blue nanocomposite. *Anal Biochem*. 2012;422:22-27.
169. Park S, Dikin DA, Nguyen ST, Ruoff RS. Graphene oxide sheets chemically cross-linked by polyallylamine. *J Phys Chem C*. 2009;113:15801-15804.
170. Yun JS, Yang KS, Kim DH. Multifunctional polydiacetylene-Graphene nanohybrids for biosensor application. *J Nanosci Nanotechnol*. 2011;11:5663-5669.
171. Liu S, Xing X, Yu J, et al. A novel label-free electrochemical aptasensor based on graphene-polyaniline composite film for dopamine determination. *Biosens Bioelectron*. 2012;36:186-191.
172. Song W, Li DW, Li YT, Li Y, Long YT. Disposable biosensor based on graphene oxide conjugated with tyrosinase assembled gold nanoparticles. *Biosens Bioelectron*. 2011;26:3181-3186.
173. Jayakumar K, Rajesh R, Dharuman V, Venkatasan R, Hahn JH, Pandian SK. Gold nano particle decorated graphene core first generation PAMAM dendrimer for label free electrochemical DNA hybridization sensing. *Biosens Bioelectron*. 2012;31:406-412.
174. Du M, Yang T, Li X, Jiao K. Fabrication of DNA/graphene/polyaniline nanocomplex for label-free voltammetric detection of DNA hybridization. *Talanta*. 2012;88:439-444.
175. Hua L, Wu X, Wang R. Glucose sensor based on an electrochemical reduced graphene oxide-poly (l-lysine) composite film modified GC electrode. *Analyst*. 2012;137:5716-5719.
176. Ang PK, Jaiswal M, Lim CH, et al. A bioelectronic platform using a graphene-lipid bilayer interface. *ACS Nano*. 2010;4:7387-7394.
177. Todakar A, Shetti NP, Devarushi US, Tuwar SM. Electro oxidation and analytical applications of valacyclovir at reduced graphene oxide modified carbon paste electrode. *Mater Today Proc*. 2019;18:550-557.
178. Unnikrishnan B, Palanisamy S, Chen S-M. A simple electrochemical approach to fabricate a glucose biosensor based on graphene-glucose oxidase biocomposite. *Biosens Bioelectron*. 2013;39:70-75.
179. Shan C, Yang H, Han D, Zhang Q, Ivaska A, Niu L. Graphene/AuNPs/chitosan nanocomposites film for glucose biosensing. *Biosens Bioelectron*. 2010;25: 1070-1074.
180. Kang X, Wang J, Wu H, Aksay IA, Liu J, Lin Y. Glucose oxidase-graphene-chitosan modified electrode for direct electrochemistry and glucose sensing. *Biosens Bioelectron*. 2009;25:901-905.
181. Wang L, Zhang X, Xiong H, Wang S. A novel nitromethane biosensor based on biocompatible conductive redox graphene-chitosan/hemoglobin/graphene/room temperature ionic liquid matrix. *Biosens Bioelectron*. 2010;26:991-995.
182. Zhao XH, Kong RM, Zhang XB, et al. Graphene-DNAzyme based biosensor for amplified fluorescence "turn-on" detection of Pb<sup>2+</sup> with a high selectivity. *Anal Chem*. 2011;83:5062-5066.
183. Dong H, Zhu Z, Ju H, Yan F. Triplex signal amplification for electrochemical DNA biosensing by coupling probe-gold nanoparticles-graphene modified electrode with enzyme functionalized carbon sphere as tracer. *Biosens Bioelectron*. 2012;33:228-232.
184. Wang J, Han H, Jiang X, Huang L, Chen L, Li N. Quantum dot-based near-infrared electrochemiluminescent immunosensor with gold nanoparticle-graphene nanosheet hybrids and silica nanospheres double-assisted signal amplification. *Anal Chem*. 2012;84:4893-4899.
185. Huang Y, Dong X, Shi Y, Li CM, Li LJ, Chen P. Nanoelectronic biosensors based on CVD grown graphene. *Nanoscale*. 2010;2:1485-1488.
186. Ohno Y, Maehashi K, Matsumoto K. Chemical and biological sensing applications based on graphene field-effect transistors. *Biosens Bioelectron*. 2010;26: 1727-1730.
187. Ohno Y, Maehashi K, Matsumoto K. Label-free biosensors based on aptamer-modified graphene field-effect transistors. *J Am Chem Soc*. 2010;132:18012-18013.
188. Kwon OS, Park SJ, Hong JY, et al. Flexible FET-type VEGF aptasensor based on nitrogen-doped graphene converted from conducting polymer. *ACS Nano*. 2012;6:1486-1493.
189. Kwak YH, Choi DS, Kim YN, et al. Flexible glucose sensor using CVD-grown graphene-based field effect transistor. *Biosens Bioelectron*. 2012;37:82-87.
190. Mao S, Yu K, Chang J, Steeber DA, Ocola LE, Chen J. Direct growth of vertically-oriented graphene for field-effect transistor biosensor. *Sci Rep*. 2013;3:1-6.
191. Dong X, Long Q, Wang J, et al. A graphene nanoribbon network and its biosensing application. *Nanoscale*. 2011;3:5156-5160.
192. Stine R, Robinson JT, Sheehan PE, Tamanaha CR. Real-time DNA detection using reduced graphene oxide field effect transistors. *Adv Mater*. 2010;22: 5297-5300.
193. Ping J, Wang Y, Fan K, Wu J, Ying Y. Direct electrochemical reduction of graphene oxide on ionic liquid doped screen-printed electrode and its electrochemical biosensing application. *Biosens Bioelectron*. 2011;28:204-209.
194. Wu S, Duan N, Ma X, et al. Multiplexed fluorescence resonance energy transfer aptasensor between upconversion nanoparticles and graphene oxide for the simultaneous determination of mycotoxins. *Anal Chem*. 2012;84:6263-6270.
195. Hong BJ, An Z, Compton OC, Nguyen ST. Tunable biomolecular interaction and fluorescence quenching ability of graphene oxide: application to "turn-on" DNA sensing in biological media. *Small*. 2012;8:2469-2476.
196. Chen Q, Wei W, Lin J-M. Homogeneous detection of concanavalin A using pyrene-conjugated maltose assembled graphene based on fluorescence resonance energy transfer. *Biosens Bioelectron*. 2011;26:4497-4502.
197. Lu CH, Li J, Zhang XL, et al. General approach for monitoring peptide-protein interactions based on graphene-peptide complex. *Anal Chem*. 2011;83: 7276-7282.
198. Lim SY, Ahn J, Lee JS, Kim MG, Park CB. Graphene-oxide-based immunosensing through fluorescence quenching by peroxidase-catalyzed polymerization. *Small*. 2012;8:1994-1999.
199. Xing XJ, Liu XG, Luo QY, Tang HW, Pang DW. Graphene oxide based fluorescent aptasensor for adenosine deaminase detection using adenosine as the substrate. *Biosens Bioelectron*. 2012;37:61-67.
200. Gao Y, Li Y, Zou X, Huang H, Su X. Highly sensitive and selective detection of biothiols using graphene oxide-based "molecular beaco"-like fluorescent probe. *Anal Chim Acta*. 2012;731:68-74.
201. Chang H, Tang L, Wang Y, Jiang J, Li J. Graphene fluorescence resonance energy transfer aptasensor for the thrombin detection. *Anal Chem*. 2010;82: 2341-2346.
202. Liu F, Choi JY, Seo TS. Graphene oxide arrays for detecting specific DNA hybridization by fluorescence resonance energy transfer. *Biosens Bioelectron*. 2010;25:2361-2365.
203. Chen JL, Yan XP, Meng K, Wang SF. Graphene oxide based photoinduced charge transfer label-free near-infrared fluorescent biosensor for dopamine. *Anal Chem*. 2011;83:8787-8793.
204. Dong H, Zhang J, Ju H, et al. Highly sensitive multiple microRNA detection based on fluorescence quenching of graphene oxide and isothermal strand-displacement polymerase reaction. *Anal Chem*. 2012;84:4587-4593.
205. Cao L, Cheng L, Zhang Z, et al. Visual and high-throughput detection of cancer cells using a graphene oxide-based FRET aptasensing microfluidic chip. *Lab Chip*. 2012;12:4864-4869.
206. Haque AM, Park H, Sung D, Jon S, Choi SY, Kim K. An electrochemically reduced graphene oxide-based electrochemical immunosensing platform for ultrasensitive antigen detection. *Anal Chem*. 2012;84:1871-1878.
207. Guo Z, Hao T, Duan J, Wang S, Wei D. Electrochemiluminescence immunosensor based on graphene-CdS quantum dots-agarose composite for the ultrasensitive detection of alpha fetoprotein. *Talanta*. 2012;89:27-32.
208. Luo M, Chen X, Zhou G, et al. Chemiluminescence biosensors for DNA detection using graphene oxide and a horseradish peroxidase-mimicking DNAzyme. *Chem Commun*. 2012;48:1126-1128.
209. Liu X, Aizen R, Freeman R, Yehezkeili O, Willner I. Multiplexed aptasensors and amplified DNA sensors using functionalized graphene oxide: application for logic gate operations. *ACS Nano*. 2012;6:3553-3563.
210. Tu W, Wang W, Lei J, Deng S, Ju H. Chemiluminescence excited photoelectrochemistry using graphene-quantum dots nanocomposite for biosensing. *Chem Commun*. 2012;48:6535-6537.
211. Bi S, Zhao T, Luo B. A graphene oxide platform for the assay of biomolecules based on chemiluminescence resonance energy transfer. *Chem Commun*. 2012;48:106-108.

212. Deng S, Lei J, Cheng L, Zhang Y, Ju H. Amplified electrochemiluminescence of quantum dots by electrochemically reduced graphene oxide for nanobiosensing of acetylcholine. *Biosens Bioelectron.* 2011;26:4552-4558.
213. Cheng Y, Yuan R, Chai Y, et al. Highly sensitive luminol electrochemiluminescence immunosensor based on ZnO nanoparticles and glucose oxidase decorated graphene for cancer biomarker detection. *Anal Chim Acta.* 2012;745:137-142.
214. Nair RR, Wu HA, Jayaram PN, Grigorieva IV, Geim AK. Unimpeded permeation of water through helium-leak-tight graphene-based membranes. *Science.* 2012;335:442-444.
215. Wang L, Zhu C, Han L, Jin L, Zhou M, Dong S. Label-free, regenerative and sensitive surface plasmon resonance and electrochemical aptasensors based on graphene. *Chem Commun.* 2011;47:7794-7796.
216. Giovanni M, Poh HL, Ambrosi A, et al. Noble metal (Pd, Ru, Rh, Pt, Au, Ag) doped graphene hybrids for electrocatalysis. *Nanoscale.* 2012;4:5002-5008.
217. Zhiguo G, Shuping Y, Zaijun L, et al. An ultrasensitive hydrogen peroxide biosensor based on electrocatalytic synergy of graphene-gold nanocomposite, CdTe-CdS core-shell quantum dots and gold nanoparticles. *Anal Chim Acta.* 2011;701:75-80.
218. Tanisell S, Arshad MM, Gopinath SC. Graphene-based electrochemical biosensors for monitoring noncommunicable disease biomarkers. *Biosens Bioelectron.* 2019;130:276-292.
219. Zhang B, Tang D, Liu B, Chen H, Cui Y, Chen G. GoldMag nanocomposite-functionalized graphene sensing platform for one-step electrochemical immunoassay of alpha-fetoprotein. *Biosens Bioelectron.* 2011;28:174-180.
220. Li Y, Yang WK, Fan MQ, Liu A. A sensitive label-free amperometric CEA immunosensor based on graphene-Nafion nanocomposite film as an enhanced sensing platform. *Anal Sci.* 2011;27:727-727.
221. Lian W, Liu S, Yu J, et al. Electrochemical sensor based on gold nanoparticles fabricated molecularly imprinted polymer film at chitosan-platinum nanoparticles/graphene-gold nanoparticles double nanocomposites modified electrode for detection of erythromycin. *Biosens Bioelectron.* 2012;38:163-169.
222. Su B, Tang D, Li Q, Tang J, Chen G. Gold-silver-graphene hybrid nanosheets-based sensors for sensitive amperometric immunoassay of alpha-fetoprotein using nanogold-enclosed titania nanoparticles as labels. *Anal Chim Acta.* 2011;692:116-124.
223. Han J, Zhuo Y, Chai YQ, Mao L, Yuan YL, Yuan R. Highly conducting gold nanoparticles-graphene nanohybrid films for ultrasensitive detection of carcinoembryonic antigen. *Talanta.* 2011;85:130-135.
224. Choi SH, Kim YL, Byun KM. Graphene-on-silver substrates for sensitive surface plasmon resonance imaging biosensors. *Opt Express.* 2011;19:458-466.
225. Lin L, Liu Y, Tang L, Li J. Electrochemical DNA sensor by the assembly of graphene and DNA-conjugated gold nanoparticles with silver enhancement strategy. *Analyst.* 2011;136:4732-4737.
226. Wan Y, Wang Y, Wu J, Zhang D. Graphene oxide sheet-mediated silver enhancement for application to electrochemical biosensors. *Anal Chem.* 2011;83:648-653.
227. Qu F, Lu H, Yang M, Deng C. Electrochemical immunosensor based on electron transfer mediated by graphene oxide initiated silver enhancement. *Biosens Bioelectron.* 2011;26:4810-4814.
228. Lu W, Luo Y, Chang G, Sun X. Synthesis of functional SiO<sub>2</sub>-coated graphene oxide nanosheets decorated with Ag nanoparticles for H<sub>2</sub>O<sub>2</sub> and glucose detection. *Biosens Bioelectron.* 2011;26:4791-4797.
229. Mena B, Miyagawa Y, Takahashi M, et al. Bioencapsulation of apomyoglobin in nanoporous organosilica sol-gel glasses: influence of the siloxane network on the conformation and stability of a model protein. *Biopolymers.* 2009;91: 895-906.
230. Qiu JD, Shi L, Liang RP, Wang GC, Xia XH. Controllable deposition of a platinum nanoparticle ensemble on a polyaniline/graphene hybrid as a novel electrode material for electrochemical sensing. *Chem Eur J.* 2012;18:7950-7959.
231. Sun W, Li L, Lei B, et al. Fabrication of graphene-platinum nanocomposite for the direct electrochemistry and electrocatalysis of myoglobin. *Mater Sci Eng C.* 2013;33:1907-1913.
232. Xiao F, Li Y, Gao H, Ge S, Duan H. Growth of coral-like PtAu-MnO<sub>2</sub> binary nanocomposites on free-standing graphene paper for flexible nonenzymatic glucose sensors. *Biosens Bioelectron.* 2013;41:417-423.
233. Shi J, Zhang H, Snyder A, et al. An aqueous media based approach for the preparation of a biosensor platform composed of graphene oxide and Pt-black. *Biosens Bioelectron.* 2012;38:314-320.
234. Bai L, Yuan R, Chai Y, Zhuo Y, Yuan Y, Wang Y. Simultaneous electrochemical detection of multiple analytes based on dual signal amplification of single-walled carbon nanotubes and multi-labeled graphene sheets. *Biomaterials.* 2012;33: 1090-1096.
235. Guo S, Wen D, Zhai Y, Dong S, Wang E. Platinum nanoparticle ensemble-on-graphene hybrid nanosheet: one-pot, rapid synthesis, and used as new electrode material for electrochemical sensing. *ACS Nano.* 2010;4:3959-3968.
236. Jang HD, Kim SK, Chang H, Roh KM, Choi JW, Huang J. A glucose biosensor based on TiO<sub>2</sub>-graphene composite. *Biosens Bioelectron.* 2012;38:184-188.
237. Huang KJ, Li J, Wu YY, Liu YM. Amperometric immunobiosensor for  $\alpha$ -fetoprotein using Au nanoparticles/chitosan/TiO<sub>2</sub>-graphene composite based platform. *Bioelectrochemistry.* 2013;90:18-23.
238. Wang K, Liu Q, Dai L, et al. A highly sensitive and rapid organophosphate biosensor based on enhancement of CdS-decorated graphene nanocomposite. *Anal Chim Acta.* 2011;695:84-88.
239. Shiddiky MJ, Rauf S, Kithva PH, Trau M. Graphene/quantum dot bionanocomposites as signal amplifiers in stripping voltammetric detection of EpCAM biomarkers. *Biosens Bioelectron.* 2012;35:251-257.
240. Zhao X, Zhou S, Jiang LP, Hou W, Shen Q, Zhu JJ. Graphene-CdS nanocomposites: facile one-step synthesis and enhanced photoelectrochemical cytosensing. *Chem Eur J.* 2012;18:4974-4981.
241. Wang K, Li HN, Wu J, et al. TiO<sub>2</sub>-decorated graphene nanohybrids for fabricating an amperometric acetylcholinesterase biosensor. *Analyst.* 2011;136: 3349-3354.
242. Lu LM, Li HB, Qu F, Zhang XB, Shen GL, Yu RQ. In situ synthesis of palladium nanoparticle-graphene nanohybrids and their application in nonenzymatic glucose biosensors. *Biosens Bioelectron.* 2011;26:3500-3504.
243. Zeng Q, Cheng JS, Liu XF, Bai HT, Jiang JH. Palladium nanoparticle/chitosan-grafted graphene nanocomposites for construction of a glucose biosensor. *Biosens Bioelectron.* 2011;26:3456-3463.
244. Ye D, Luo L, Ding Y, Liu B, Liu X. Fabrication of Co<sub>3</sub>O<sub>4</sub> nanoparticles-decorated graphene composite for determination of L-tryptophan. *Analyst.* 2012;137:2840-2845.
245. Wang Y, Yuan R, Chai Y, Yuan Y, Bai L, Liao Y. A multi-amplification aptasensor for highly sensitive detection of thrombin based on high-quality hollow CoPt nanoparticles decorated graphene. *Biosens Bioelectron.* 2011;30:61-66.
246. Venkatesan BM, Estrada D, Banerjee S, et al. Stacked graphene-Al<sub>2</sub>O<sub>3</sub> nanopore sensors for sensitive detection of DNA and DNA-protein complexes. *ACS Nano.* 2012;6:441-450.
247. Mena F, Mena B, Sharts O. Development of carbon-fluorine spectroscopy for pharmaceutical and biomedical applications. *Faraday Discuss.* 2011;149: 269-278.
248. Mena F, Mena B, Sharts ON. Spectro-Fluor™ technology for reliable detection of proteins and biomarkers of disease: a pioneered research study. *Diagnostics (Basel).* 2014;4:140-152.
249. Sharts CM, Gorelik VS. Method and apparatus for determination of carbon-halogen compounds and applications thereof. *Google patents.* 2002.
250. Ling X, Xie L, Fang Y, et al. Can graphene be used as a substrate for Raman enhancement? *Nano Lett.* 2010;10:553-561.
251. Ling X, Fang W, Lee YH, et al. Raman enhancement effect on two-dimensional layered materials: graphene, h-BN and MoS<sub>2</sub>. *Nano Lett.* 2014;14:3033-3040.
252. Silver A, Kitadai H, Liu H, et al. Chemical and bio sensing using graphene-enhanced Raman spectroscopy. *Nanomaterials.* 2019;9:516.
253. Ling X, Huang S, Kong J, Dresselhaus M. Graphene-enhanced Raman scattering (GERS): chemical effect. In: Kneipp K, Ozaki Y, Tian Z-Q (eds) *Recent Developments in Plasmon-Supported Raman Spectroscopy.* 2017:512.
254. Chen Y, Zhang Y, Pan F, et al. Breath analysis based on surface-enhanced Raman scattering sensors distinguishes early and advanced gastric cancer patients from healthy persons. *ACS Nano.* 2016;10:8169-8179.